



# Fundamentals of Geometric Construction

Paul Zsombor-Murray

► **To cite this version:**

Paul Zsombor-Murray. Fundamentals of Geometric Construction. Engineering school. McGill University, 2007. <cel-00365579>

**HAL Id: cel-00365579**

**<https://cel.archives-ouvertes.fr/cel-00365579>**

Submitted on 3 Mar 2009

**HAL** is a multi-disciplinary open access archive for the deposit and dissemination of scientific research documents, whether they are published or not. The documents may come from teaching and research institutions in France or abroad, or from public or private research centers.

L'archive ouverte pluridisciplinaire **HAL**, est destinée au dépôt et à la diffusion de documents scientifiques de niveau recherche, publiés ou non, émanant des établissements d'enseignement et de recherche français ou étrangers, des laboratoires publics ou privés.

# MECH 289 Design Graphics Fundamentals of Geometric Construction

7th March 2007

(MECH289)M2DG289LC

## 1 Module M2

- This module is designated “Fundamentals of geometric construction”.
- It is composed of six topics, each of which will be dealt with in a week of lectures, *i.e.*, in three 50 minute or two 80 minute periods. These topics are enumerated below.
  1. Point, plane, polygon and platonic
  2. Geometry in mechanics
  3. Symmetry and solid modelling
  4. Quadric surfaces and their intersection
  5. Parametric curves and surfaces
  6. Connecting two lines with a third

These topics are meant as examples to stimulate “geometric thinking”. This facility is especially important in design however it is overlooked or absent in many engineering courses.

## 2 Point, Plane, Polygon and Platonic

In this and subsequent sections we will draw heavily on procedures from classical descriptive geometry (DIG) because it is felt that multiview parallel projection is an invaluable tool in conceptual design and visualization and interpretation of combinations of numerous solid elements that have many metric and symmetric properties. In this course we will do some DIG exercises in a CAD environment because CAD construction, unlike manual drafting, produces precise results.

### 2.1 Descriptive Geometry Topics

(not necessarily in order nor covered extensively)

1. Coordinate system & principal views of points, lines & planes
2. Principal lines & planes
3. Alternate plane definitions
4. Slope, bearing & true length of a line segment
5. Point (end) view of a line
6. Line (edge) view of a plane
7. True view (shape) of a plane
8. Slope, strike & dip direction (bearing) of sloping plane
9. Principal piercing points of a line
10. Lines parallel & perpendicular to planes & other lines
11. Planes which are mutually parallel or perpendicular
12. Containment of a point on a plane
13. Distance (shortest) from point to plane
14. Piercing point (trace or intersection) of line & plane
15. Projection of point onto a plane
16. Angle between line & plane
17. Angle between two lines
18. Line of intersection (trace) between two planes

19. Dihedral angle between two planes
20. Line joining two skew lines (See section 7)
21. Developments & intersections of planar and quadric surfaces (See section 4)
22. Vector statics (Concurrent forces & Maxwell diagram, see section 3.3)
23. Earthworks and excavations

DIG is a constructive (by making drawings) tool to extract quantitative (distances and angles, areas and volumes, *etc.*) information (answers) from engineering designs (of buildings, structures, earthworks or machines) represented by geometric models of physical objects.

## 2.2 Elements

(Linear) modelling elements, in 3D Euclidean space, which concern us are:-

- Points
- Lines
- Planes

While we will also examine some second order surfaces or *quadrics* which include:-

- Cylinder of revolution
- Cone of revolution
- Sphere

We will merely touch on the other quadrics:-

- General cylinder and cone
- Ellipsoid
- Paraboloid
- Hyperbolic paraboloid
- Hyperbolæ of one and two sheets

However, if time permits, we may mention some interesting fourth order surfaces:-

- Torus
- Cyclide
- Conoid

These are important in the design of elegant, modern buildings based on advanced architectural concepts which include structural elements which may be intermittently or continuously mobile. *E.g.*, the celebrated engineer-architect, Santiago Calatrava, designs building rib systems based on the skeletal anatomy of birds. One of his recent (ongoing) projects is a new building at Ryerson Technical University in Toronto. It has a wall that undulates with a travelling wave of ribs that swing on a common longitudinal axis. Hunt this up on the web if you're interested.

### 2.3 Combination and Intersection

Look at the 23 numbered topics in section 2.1. Aside from construction for *measurements* like true length of a line segment or angle between two lines, two planes or a line and a plane, most of the topics and exercises pertain to *combinations* of elements to form structures and the consideration of the nature of element *intersections*. This is useful in designing the elements so that they go together and fit properly. This also applies to “holes” which must be dug to accept a structure like a tunnel or foundation. Before going on to do exercises, related to measurement, combination and intersection, certain basic definitions and concepts will be introduced and discussed.

### 2.4 The Principal Frame

Consider Fig. 1. As shown there, a conventional Cartesian coordinate system is embedded in a “box”, 24 units on every edge. The origin  $O$  is on the near upper left corner and the principal axes,  $x, y, z$ , are shown along three box edges. In the “pictorial” on the left one sees the given point  $A(10, 6, -8)$  “frozen” in the box as if it were a block of ice. Also seen are three dotted lines on  $A$ , respectively perpendicular to principal viewing planes  $H(x, y)$ ,  $F(z, x)$  and  $P(y, z)$ , which connect to the projections or images of  $A$  on these planes, *i.e.*,  $A_H$ ,  $A_F$  and  $A_P$ , respectively. One generally uses negative  $z$ -coordinates and positive  $y$ - and  $x$ -coordinates to keep top and front views separate in a drawing.

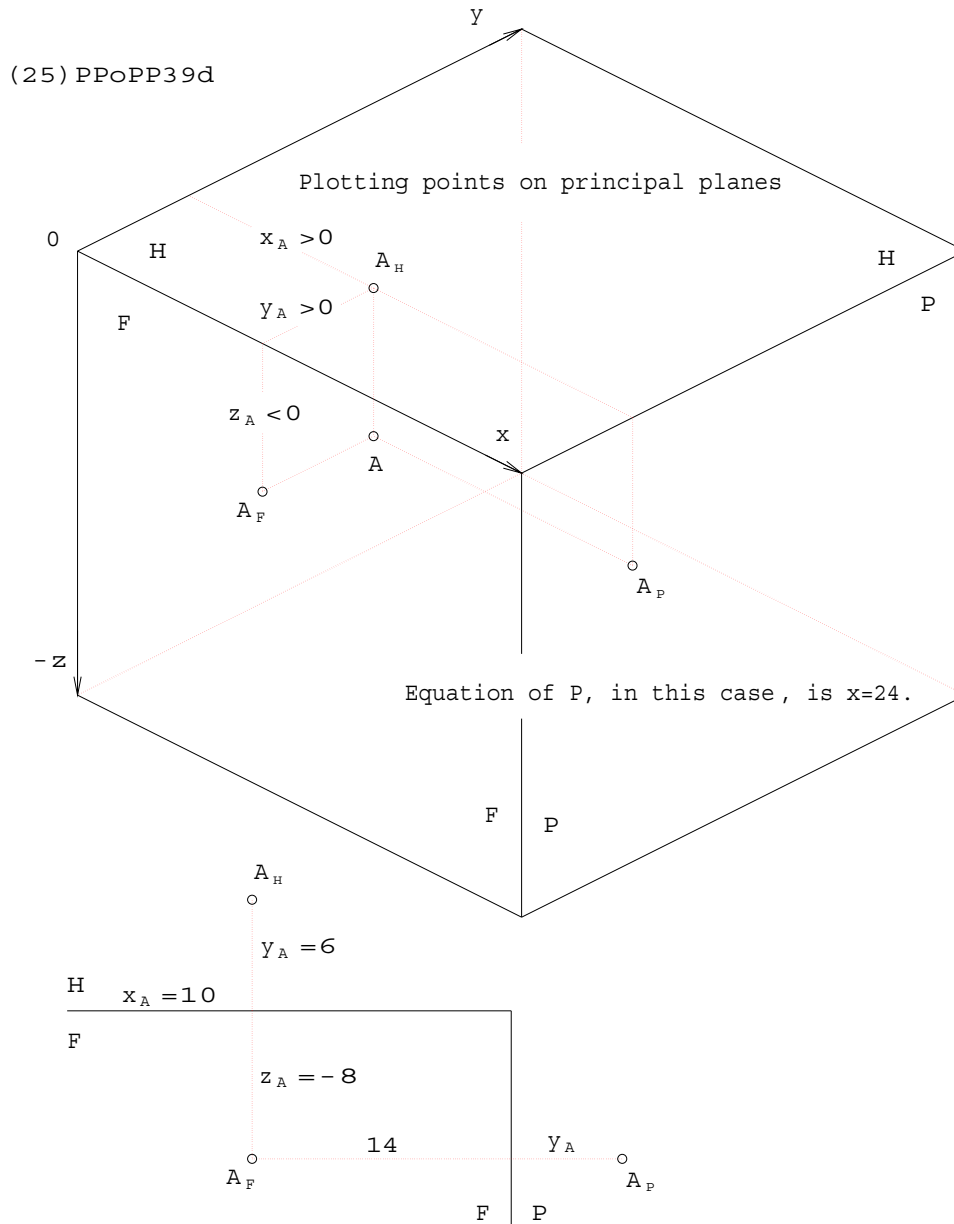


Figure 1: Points on Principal Planes

In descriptive geometry one does not use pictorial representation, rather a pair of *conjugate* views are regarded simultaneously. Imagine the left eye sees plane  $H$  from so far away in the  $z$ -direction that all lines, connecting points in the box like  $A$  to  $A_H$ , appear as points. Similarly, the right eye sees the image of  $A$  on  $A_F$  because that eye is located at  $y \rightarrow -\infty$ . The descriptive geometric representation of  $A$  appears in the right hand illustration. The left eye sees  $A$  on  $A_H$  and the plane  $F$ , the front of the box, appears as the line  $\frac{H}{F}$ . Conversely the right eye sees  $A_F$  and the top of the box becomes the line  $\frac{H}{F}$ . The dotted line joining  $A_H$  and

$A_F$  is in fact two lines which are in fact *not* collinear, not even parallel, but perpendicular, as can be seen in the pictorial. The top,  $H$ , and front,  $F$ , views are called a *conjugate view pair*. The  $x, y$  coordinates are measured in  $H$  and the  $x, z$  coordinates are measured in  $F$ . The redundant  $x$ -coordinate is common or conjugate.

As an exercise, rewrite the paragraph above to describe the conjugate view pair  $\frac{F}{P}$ . Consider that the  $P$  view is obtained by rotating the left eye about the viewing axis of the stationary right eye. This axis is parallel to the  $y$ -axis. The rotation is positive in the sense of a right-hand screw. To see the  $P$  or right side view, the left eye thus moves from  $z \rightarrow +\infty$  to  $x \rightarrow +\infty$ . No new information is generated by the  $P$  view or projection. Therefore it is a so-called “auxiliary view”, albeit a special one involving a rotation of  $\frac{\pi}{2}$ . As a second concept familiarization exercise, write out how to move an eye-ball to obtain conjugate view pairs which show the other three box faces, *i.e.*, left-side, bottom and rear. General auxiliary views are obtained by rotations which are not multiples of  $\frac{\pi}{2}$ . Generation of auxiliary views is a primary descriptive geometry problem-solving tool. It will be dealt with soon.

## 2.5 Points, Lines and Planes in Three-Dimensional Space

The following itemized lists must be learned. The purpose and application of the items must be understood in order to acquire skill in “geometric thinking”. The physical objects engineers encounter, design and build are usually conceived, manipulated and communicated as images. We must have means to do this so as to *complement* the conventional mathematical modelling through algebraic and differential equations studied by engineers.

### 2.5.1 Shorthand

- (=) means “parallel to”
- (+) means “perpendicular to”
- ( $\approx$ ) means “not parallel to”
- ( $\pm$ ) means “not perpendicular to”
- (#) means “neither (=) nor (+)”
- (e/l) means “edge/line view of plane”
- (e/p) means “end/point view of line”
- (v/p) means “view/projection”
- (TL) means “true length” (of a line segment can be measured)
- (TA) means “true angle” (between lines or planes or one of each can be measured)

- (TS) means “true shape” (on a plane (+) viewing axis; an enclosed area can be measured)
- (LoX) means “line of intersection” (on two planes)

### 2.5.2 Properties of Principal Projections of Points & Lines

1. The distance from a point to a plane is measured (+)(e/l)
2. (e/l)H appears in (v/p)F
3. (e/l)F appears in (v/p)H and (v/p)P
4. (e/l)P appears in (v/p)F
5. A line can be detected (=) a plane in any(v/p) showing (e/l)
6. The (TL) of a line is visible and measurable in any (v/p) to which the line is (=)
7. The (TA) between a line and plane is visible in any (v/p) where the line appears (TL) and the plane appears (e/l)
8. A plane (+) any (v/p) appears (e/l)
9. A line (+) any (v/p) appears (e/p)
10. A line appearing as (e/p) is (=) to every other line in (e/p) and is (=) to every plane in (e/l) which appear in that (v/p)

### 2.5.3 Plane Definitions

1. 3 given points,  $ABC$
2. A line,  $AB$ , and a point,  $C$
3. A pair of intersecting lines,  $AB$  and  $BC$
4. A pair of principal traces,  $HS$  and  $FS$ .
5. A slope line,  $BG$
6. A pair of (=) lines



## 2.5.4 Plane/Line Properties

- A plane,  $ABC$ , is (=) to a line,  $LM$ , if  $LM$  is (=) *any* line, say  $AC$ , in the plane.
- A plane,  $ABC$ , is (+) to a line,  $JK$ , if  $JK(+)$  to *all* lines in  $ABC$ . Two lines, ( $\approx$ ) to each other will do, say  $AD$  and  $AE$ .
- 2 lines are (+) if one is in (TL) and they appear (+).
- 2 lines are (=) each other if they appear (=) in an adjacent or conjugate pair of (v/p).
- The slope of a plane is the slope of its slope line.
- The slope angle of a plane is visible when it appears (e/l) together with (e/l)H in any (v/p).
- An (e/l) is visible in any (v/p)(+) to any line in the plane.
- An (e/l) is visible in any (v/p) showing (e/p) in the plane.

As a preliminary free-hand sketching exercise, clarify every statement in [2.5.2](#) through [2.5.4](#) with a neat little illustration.

## 2.6 Interpreting Element Properties

Fig. [2](#) and Fig. [3](#) require some explanation. They describe principal view discernable descriptive geometric property relationships among linear elements, *i.e.*, P=point, N=plane, L=line, *e.g.*, PP=point-point, LN=line-plane, *etc.*. (D) means a measurable distance, (ON) means literally “on”, *i.e.*, as in a point is on a line. It is by studying, learning and using these “direct method” relationships that you will begin to understand and appreciate descriptive geometry.

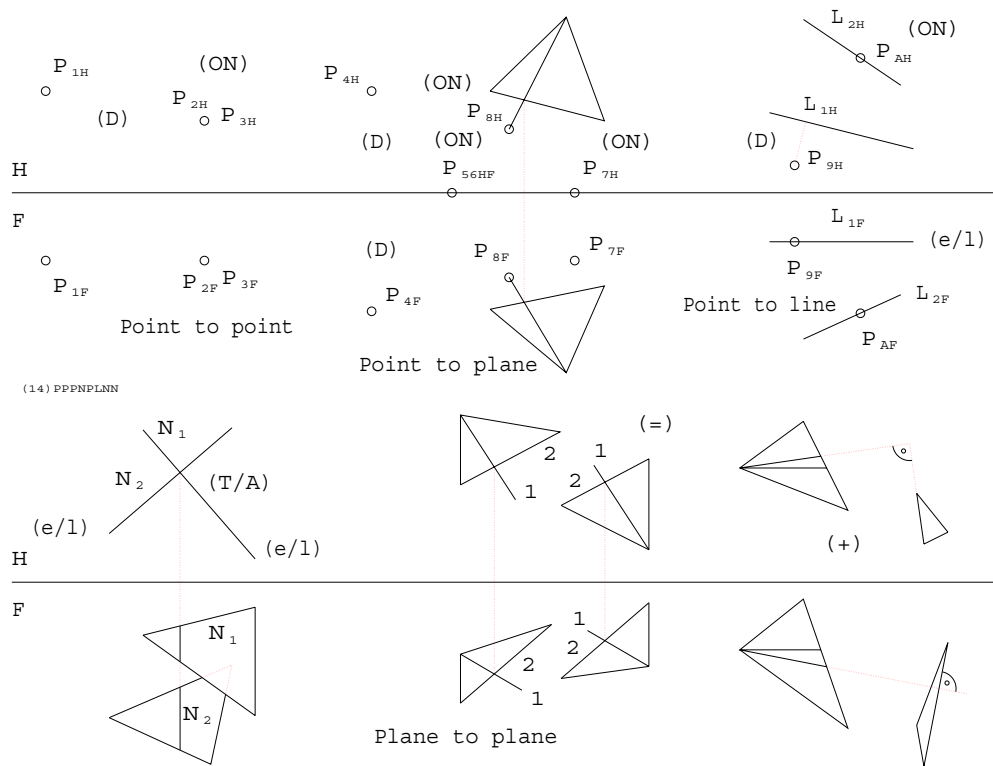


Figure 2: Relations: Point to Point, Point to Plane, Point to Line and Plane to Plane

### 2.6.1 Point to Point in Fig. 2

This principal view pair shows that the distance between  $P_1$  and  $P_2$  is measurable in  $-H-$  because the segment  $P_1P_2$  is visible there. Furthermore  $P_2$  is coincident with  $P_3$  because the coincidence is visible in *both* views of a *conjugate pair*. A conjugate pair is a pair of projections on  $(+)$  ( $v/p$ ) that share a common coordinate like  $x$  is shared between  $-H-$  and  $-F-$ . The planes are sometimes shown separated by a double-edge-view line, like  $-HF-$  or  $-12-$  or another label pair.

### 2.6.2 Point to Plane in Fig. 2

Here we see the distances between  $P_4$  and the principal planes  $-H-$  and  $-F-$ . These are the respective  $z-$  and  $y-$  coordinates.  $P_5$  and  $P_6$  are coincident with each other but also lie simultaneously on the planes  $-H-$  and  $-F-$ .  $P_7$  is on  $-F-$  but a measurable distance from  $-H-$ . Note its finite  $z-$  coordinate.  $P_8$  is on plane  $N$  because  $P_8$  is on a line which in turn is on  $N$ . Why? The line is on a vertex point of a segment of  $N$ . Furthermore the line containing  $P_8$  intersects the side opposite the vertex in a point on that opposite side.

### 2.6.3 Point to Line in Fig. 2

We see the distance from  $P_9$  to  $L_1$  in -H- because  $P_9$  and  $L_1$  define a horizontal plane. Note the shorthand argument  $(e/l)N(PL)$  that means, "A point and line used to define a plane coincide with any edge/line view of that plane." Try to formulate some of these for yourself to help in recall and understanding of the essential principles. Furthermore  $P_A$  is clearly on  $L_2$  due to coincidence in both views.

### 2.6.4 Plane to Plane in Fig. 2

We see simultaneous  $(e/l)$ s of  $N_1$  and  $N_2$  in -H- because the line of intersection  $LoX$  of these two planes is a horizontal projector or frontal-profile line or vertical line; the three names are interchangeable. Since both planes are in  $(e/l)$  the  $(TA)$  between them can be measured in the -H- view. In the middle we see two plane segments. They are  $(=)$ . Why? Note that the view pairs of the lines labelled 1 and 2, which are on the respective segments, are  $(=)$ . If a plane pair contains respective pairs of  $(=)$  lines, the planes are  $(=)$ . At lower right we see the  $(+)$  relationship between two plane segments. The left hand plane contains two principal lines which are  $(+)$  to an  $(e/l)$  segment of the right hand plane so the planes are  $(+)$ . A plane is  $(+)$  to another if it contains one line which is  $(+)$  to all lines in the other.

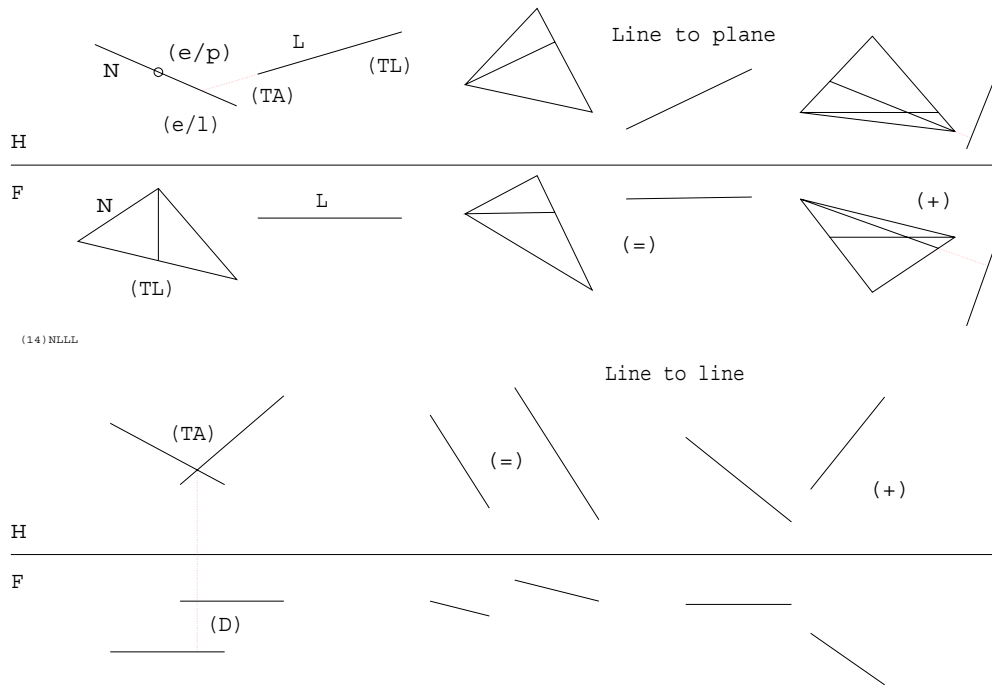


Figure 3: Relations: Plane to Line and Line to Line

### 2.6.5 Plane to Line in Fig. 3

Here we see the (TL), (TA) relationship between -F- and a horizontal line. Also shown is the simultaneous (e/l) relationship which is to be exercised in your second assignment to finally get the true shape of a plane segment. In the middle picture on top we see that a given line is (=) to a plane if the plane contains one line (=) to the given one. In the case of line/plane perpendicularity, the line must be (+) to all lines contained in the plane in question. Two will do if they are not (=). Principal lines were chosen for this demonstration because they are easy to construct and diagnosis is immediate. Note how much more difficult and inaccurate it would be if the test required two auxiliary views to see the plane in (e/l) and the line in (TL). Or would that require three auxiliaries?

### 2.6.6 Line to Line in Fig. 3

Here we see (TA) measurement between lines; both lines appear in (TL) view: Parallelism between lines; conjugate view *pairs* show parallelism, one view is not enough. Finally the perpendicularity of lines is illustrated by seeing one of the lines in (TL) view and noting the apparent 90° angle which in this case is for real.

## 2.7 Planes in Space

Examine Fig. 4. The  $24 \times 24 \times 24$  finite cube or “box” is drawn in pictorial by showing visible edges of its bounding plane faces. The box represents a finite portion of our three-dimensional (3D) Euclidean space because the entire, empty space cannot be “seen”. Also shown are two planes labelled [S] and [T]. Since these too are empty, featureless 2D domains embedded in 3D space they can only be seen by edges or lines upon them. The lines in turn are 1D spaces in 3D space which, in this case, are entirely on the planes whose edges they represent. We see the lines because they are composed of an infinite number of points in a row, shown as black dots, infinitesimally separated. Of course the dots of 0D must be represented by specks of small but finite size.

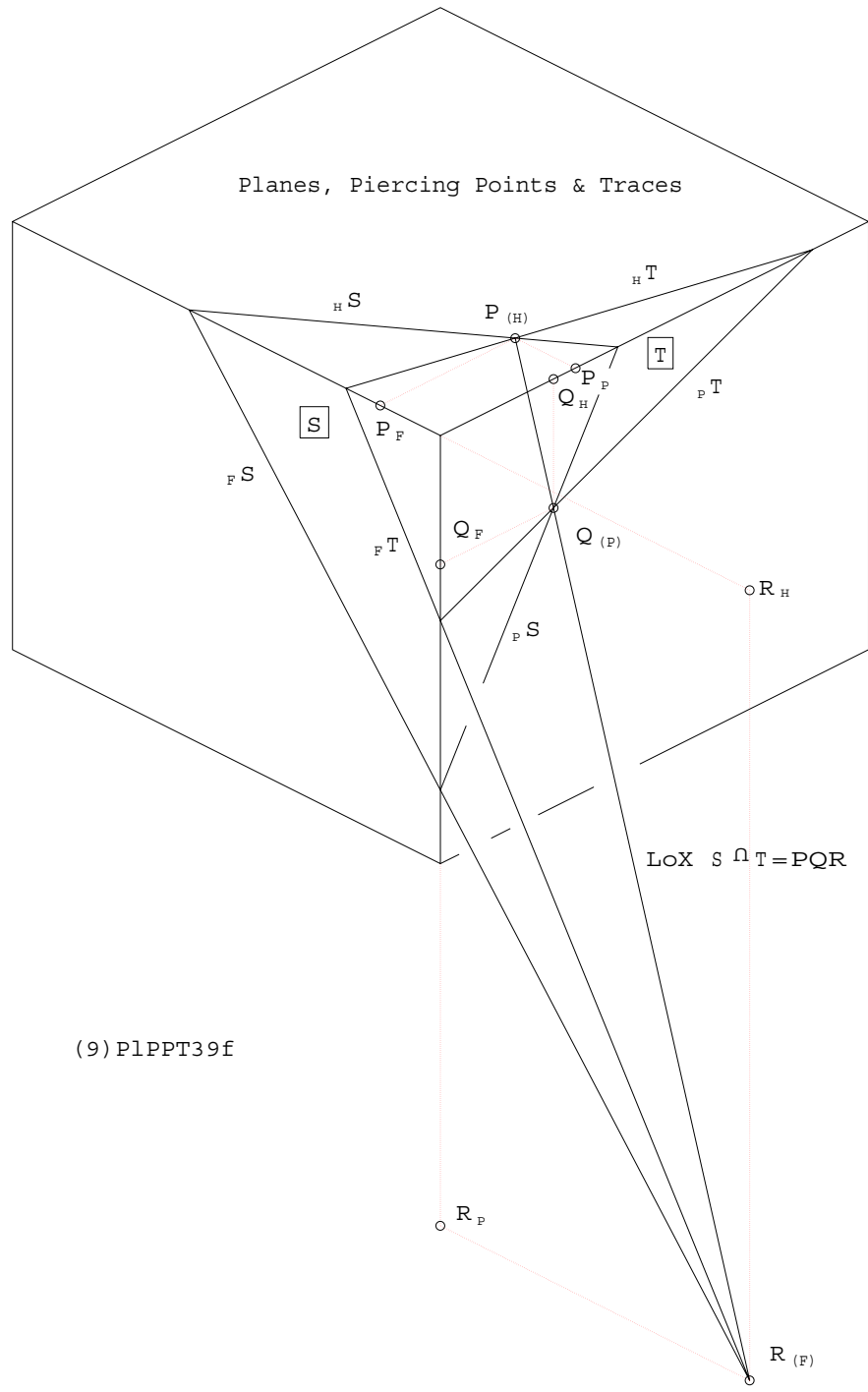


Figure 4: Piercing Points  $P, Q, R$  of  $(LoX)$  between Planes  $[S]$  and  $[T]$  Represented by Principal Traces

### 2.7.1 Traces and Piercing Points

A geometric trace (not the trace of a matrix) is the 1D intersection of two 2D spaces or surfaces. In the case of plane surfaces the trace is a line. We will be examining traces on plane pairs in some detail here. Later, we will discuss traces which are curves of intersection. *E.g.*, intersecting spheres have a circle in common. On the other hand a piercing point is the intersection of a curve and surface. In the case of plane and line there is only one piercing point. Since lines may be imagined as formed by intersecting planes, one may consider the point as common to three planes. As a mental exercise, “think geometrically” and imagine pictures:- What is the maximum number of (real) piercing points on a sphere? ... on an ellipse?

### 2.7.2 Principal Traces of General Planes

With respect to the pictorial box, plane [S] has traces  ${}_H S$ ,  ${}_F S$  and  ${}_P S$  on the principal, or coordinate planes [H], [F] and [P], respectively. Note also  ${}_H T$ ,  ${}_F T$  and  ${}_P T$  as regards plane [T].

### 2.7.3 Traces

A pair of distinct planes *always* intersects on a line.

- [H] and [F] intersect on the line  $\frac{H}{F}$
- [F] and [P] intersect on the line  $\frac{F}{P}$
- Plane [P] could have been conjugated with [H] via the top-right box edge  $\frac{H}{P}$  (not labelled) however the conjugation  $\frac{F}{P}$  is the standard convention found in North American texts.
- In addition to the six principal traces noted above, one sees line  $\frac{S}{T}$  (unlabelled), the intersection of [S] and [T]. It is on points  $P$ ,  $Q$  and  $R$ .
- Notice that  $P_{(H)} = {}_H S \cap {}_H T$ . The bracketed subscript ( $H$ ) indicates that the point  $P$  in space is coincident with its top view or horizontal projection  $P_H$  as well as being on the intersection of the two horizontal traces.
- There are two dotted, mutually (+) *projectors* or lines, respectively (+) planes [H] and [P], on  $P_{(H)}$  which locate the other two principal projections of point  $P$ . Now repeat this item and the previous one, twice, below with respect to points  $Q$  and  $R$ .
- :-
- :-

- :-
- :-

#### 2.7.4 Piercing Points

Piercing points are line-plane intersections. Here we will deal specifically with *principal* piercing points, *i.e.*, intersections of lines with *principal* planes. Fig. 5 shows, in pictorial and as a conjugate principal view pair construction, the principal piercing points of a line segment  $AB$

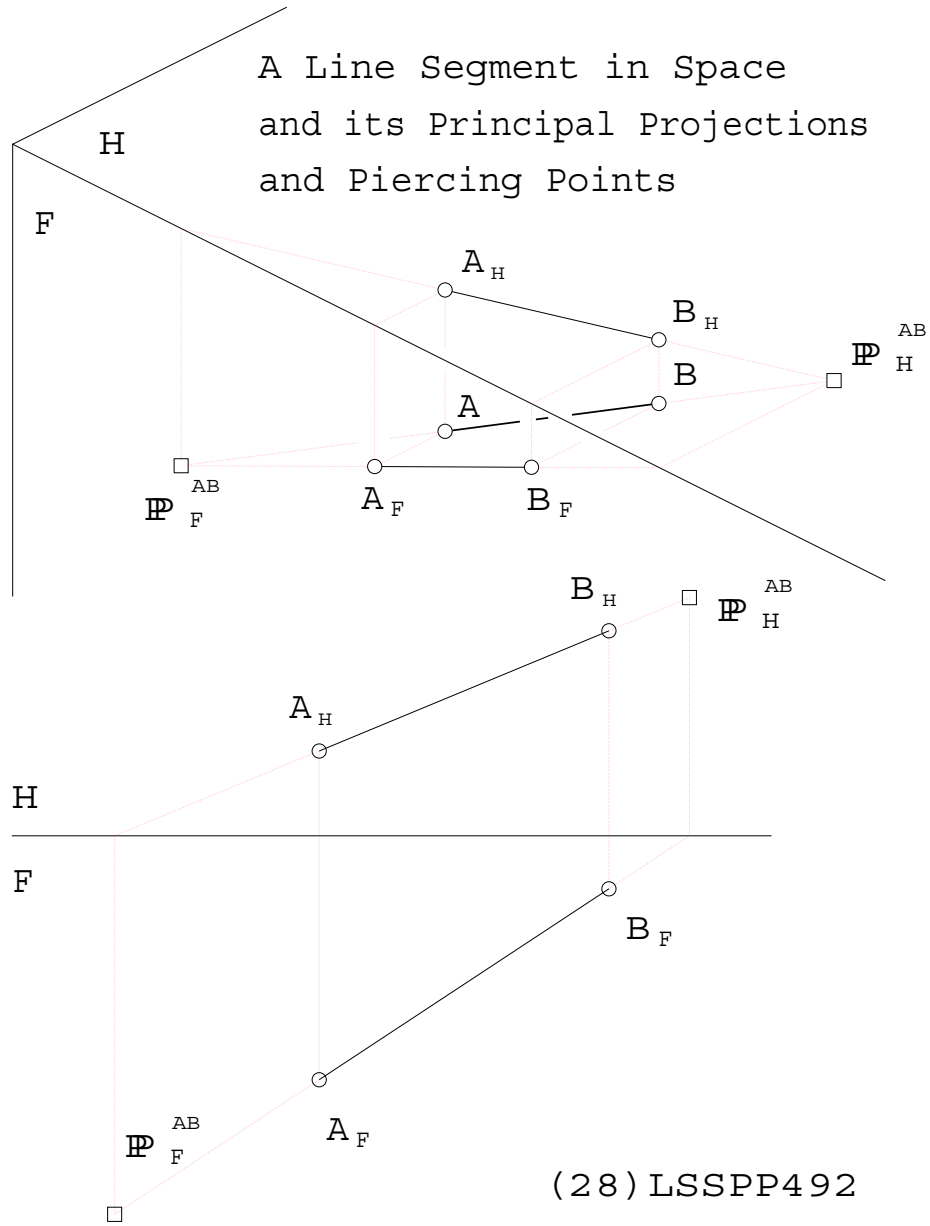


Figure 5: Principal Piercing Points of a Line Segment

- The principal line  ${}_H S$ , an edge of a plane segment of [S], intersects plane [F] on a point  $(x_S, 0, 0)$ .
- The principal line  ${}_F S$ , an edge of a plane segment of [S], intersects plane [H] on the same point. Now repeat this and the first item above five times to describe the other five principal piercing points of the remaining five principal edge-lines of the two planes [S] and [T].
- :-



- :-
- :-
- :-
- :-
- :-
- :-
- :-
- :-
- :-
- :-

- Notice that  $P_{(H)}$ ,  $Q_{(P)}$  and  $R_{(F)}$  are the three principal piercing points on the intersection  $\frac{S}{T}$ , a skew or general (not principal) line. This line is the set of points common to [S] and [T] (just like  $HS$ , for example, is the set of points common to [H] and [S]).

## 2.8 Problem Examples

Now look at Fig. 6 to see how all this insight works with an  $\frac{H}{F}$  descriptive geometric conjugate view pair. This is a direct method construction followed by Fig. 7, a more straight-forward but tedious, error-prone construction. The moral of the story:- **Geometric thinking leads to more robust, efficient computation.**

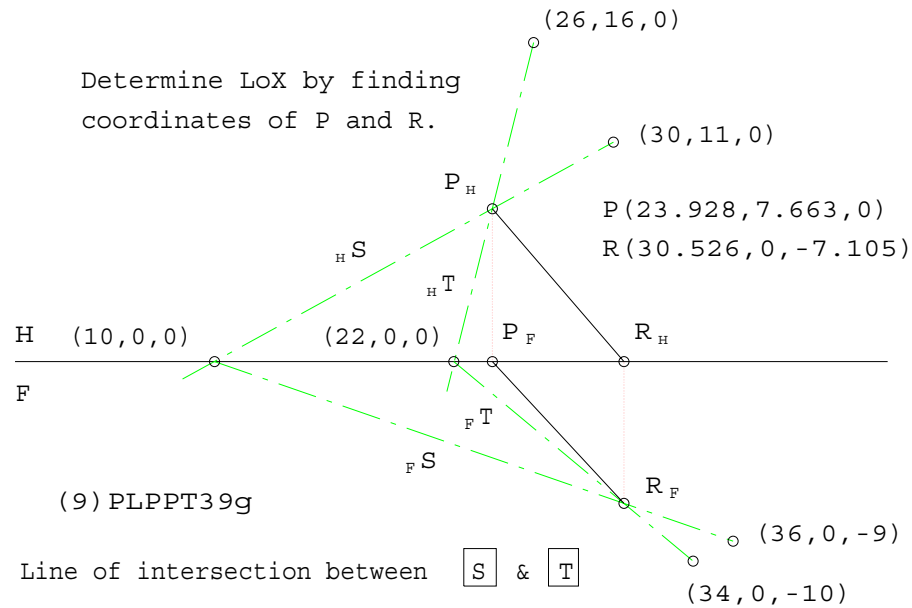


Figure 6: Intersection of Planes Using Traces

### 2.8.1 Exercises

Remember that an exercise is due every week. Do what you can and hand in what you have done by the specified noon deadline. The nice thing about CAD drawing is that you can still work on partially completed stuff that you have submitted as evidence of progress.

### 2.8.2 Exercise 1.

Reproduce Fig. 6 to find the coordinates of  $P$  and  $Q$ .

### 2.8.3 Exercise 2.

Using Fig. 6 find the true length, bearing and slope of the *five* line segments shown. (no, there are not six!) Hints:-

- Properties of the four traces can be obtained by inspection and direct measurement; no additional construction (drawing) is necessary. Where is the “missing” (v/p) of each of these four lines?
- The bearing of  $P \rightarrow R$  is measured in (v/p)H, also called the top- or plan-view. It

is a north-azimuth angle measured clockwise from north ( $\uparrow$ ) unless a compass rose is shown. In this case there is none.

- The slope of  $P \rightarrow R$  is measured from an (e/l) of [H] in a (v/p) which also shows  $PR$  as (TL). Construct an auxiliary (v/p) on plane [1] which is (+) [H] and (=)  $PR$ .

### 2.8.4 Exercise 3.

Reproduce Fig. 7 to find the coordinates of  $K$  and  $L$ . Hint:-

- In this case [1] is (+), not (=), to horizontal line segment  $AJ$ .
- Auxiliary plane [1] is of course (+) (v/p)H.
- Notice that  $K_1$  and  $L_1$  are located on the respective intersections of plane segment (e/l)  $A_1B_1C_1$  and line segments  $G_1D_1$  and  $G_1E_1$ .
- Ignore the principal conjugate (v/p) pair  $\frac{H}{F}$  for the moment. Consider it replaced by  $\frac{1}{H}$ . The “down” direction is replaced here by  $z$ -coordinates measured from (e/l)H, upwards and to the right. Imagine how “Monge’s Monster” has moved its right eye which now sees images projected onto plane [1].

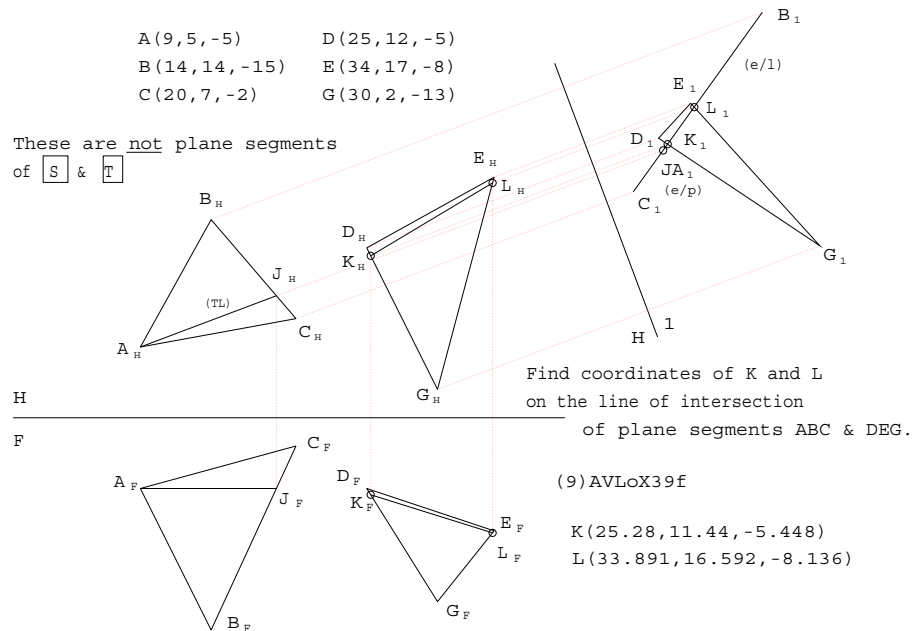


Figure 7: Line of Intersection with Auxiliary View

### 2.8.5 Relevant Linear Algebra

This seems a good place to deal analytically with some of the previous constructions and some to follow. Refer to illustrations on Fig. 8 to see the geometry behind the algebra.

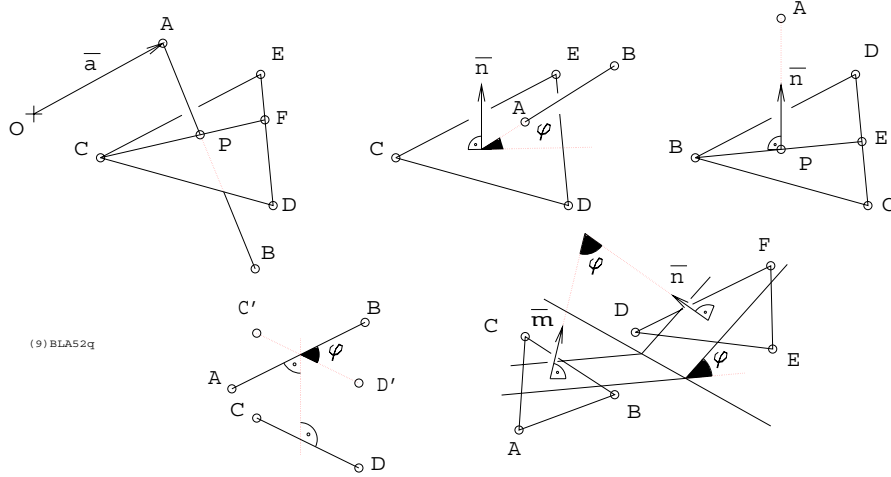


Figure 8: Basic Geometry of Points, Planes & Lines

- **Piercing Point** between line and plane is found with the three simultaneous linear equations. Note that  $\mathbf{a}$  is the position vector of point  $A$ , *etc.*, and that  $t$ ,  $u$  and  $v$  are scalar fractional distance in the interval between points, *e.g.*,  $t$  is a fraction of the length from  $\mathbf{a}$  to  $\mathbf{b}$ .

$$\begin{aligned}\mathbf{p} &= \mathbf{a} + t(\mathbf{b} - \mathbf{a}) \\ \mathbf{p} &= \mathbf{c} + u(\mathbf{f} - \mathbf{c}) \\ \mathbf{f} &= \mathbf{d} + v(\mathbf{e} - \mathbf{d})\end{aligned}\tag{1}$$

Subtracting the second of Eqs. 1 from the first and then subtracting the third, multiplied by  $u$ , from the result of the first subtraction yields Eq. 2 which can be solved for  $t$ ,  $u$  and the product  $uv$ .

$$(\mathbf{a} - \mathbf{b})t + (\mathbf{d} - \mathbf{c})u + (\mathbf{e} - \mathbf{d})uv + (\mathbf{c} - \mathbf{a})t\tag{2}$$

- **Angle between Line and Plane** is determined with unit normal  $\mathbf{n}$ .

$$\mathbf{n} = \frac{(\mathbf{d} - \mathbf{c}) \times (\mathbf{e} - \mathbf{c})}{\|\mathbf{d} - \mathbf{c}\| \|\mathbf{e} - \mathbf{c}\|}\tag{3}$$

Then the angle  $\phi$  is found as  $\sin^{-1} \phi$ .

$$\sin \phi = \frac{\mathbf{b} - \mathbf{a}}{\|\mathbf{b} - \mathbf{a}\|} \cdot \mathbf{n}\tag{4}$$

- **Projecting a Point Normally on to a Plane** begins with a normal, not necessarily unit, vector to the plane.

$$(\mathbf{c} - \mathbf{b}) \times (\mathbf{d} - \mathbf{b}) - \mathbf{n} = \mathbf{0} \quad (5)$$

Then this is reduced to a piercing point problem with the three simultaneous equations, Eqs. 6, equivalent to Eqs. 1.

$$\begin{aligned} \mathbf{p} &= \mathbf{a} + t\mathbf{n} \\ \mathbf{p} &= \mathbf{b} + u(\mathbf{e} - \mathbf{b}) \\ \mathbf{e} &= \mathbf{c} + v(\mathbf{d} - \mathbf{c}) \end{aligned} \quad (6)$$

- **Angle between Lines** is found as  $\phi$  such that

$$\cos \phi = \frac{(\mathbf{b} - \mathbf{a}) \cdot (\mathbf{d} - \mathbf{c})}{\|\mathbf{b} - \mathbf{a}\| \|\mathbf{d} - \mathbf{c}\|} \quad (7)$$

- **Angle between Planes** is found as  $\phi$  such that

$$\cos(\pi - \phi) = \mathbf{m} \cdot \mathbf{n}, \quad \mathbf{m} = \frac{(\mathbf{b} - \mathbf{a}) \times (\mathbf{c} - \mathbf{a})}{\|\mathbf{b} - \mathbf{a}\| \|\mathbf{c} - \mathbf{a}\|}, \quad \mathbf{n} = \frac{(\mathbf{e} - \mathbf{d}) \times (\mathbf{f} - \mathbf{d})}{\|\mathbf{e} - \mathbf{d}\| \|\mathbf{f} - \mathbf{d}\|} \quad (8)$$

## 2.9 Platonic Solids

These plane sided regular figures exhibit fundamental aspects of spatial symmetry. Furthermore their study will provide opportunity to use the linear algebraic equivalent to elementary descriptive geometric construction exercises. Euler's formula is pertinent because it relates edges (lines) and vertices (points) that are the consequence of face (plane) intersection in the case of solids with planar boundaries. Consider it an introduction to topology, the branch of mathematics even more general than geometry.

$$V - E + F - 2 = 0$$

or more generally

$$V - E + F - H - 2(C - G) = 0$$

Any solid bounded by plane segment facets, or faces, adheres to the above relation.  $V$  is the number of corners or vertices (points).  $E$  is the number of edges or boundary lines of intersection on two faces. The total number of faces is  $F$ .  $H$  is the number of "holes" or concavities in the surface of the solid. However the solid may be composed of disjoint, separate component pieces or "islands" numbering  $C$ .  $G$  is the "genus" of the solid.  $G$  is the number of through holes or tunnels.

### 2.9.1 Constructing Regular Polygons

**Regular Polygons**, except for those requiring angular trisection that is generally not possible, are constructed with the following tools, commonly encountered in high-school geometry.

- Dividing an interval on a line into a sequence of  $n$  equal length segments
- Bisecting an angle
- Constructing pairs of line segments that are parallel, perpendicular and at binary multiples and fractions of  $\pi/3$
- Constructing the right bisector of a line segment
- Constructing the inscribing and circumscribing circles on a triangle and finding the centroid

### 2.9.2 The Pentagon and an Introduction to the Platonics

The regular pentagon is a special case and will be dealt with when treating the twelve sided regular solid or dodecahedron, the fourth member of the five so called *platonic solids*. These are the tetrahedron $\{3, 3\}$  with four vertices and faces, cube $\{3, 4\}$  with six faces and eight vertices, octahedron $\{4, 3\}$  with six vertices and eight faces, dodecahedron $\{3, 5\}$  with twenty vertices and twelve faces and icosahedron $\{5, 3\}$  with twelve vertices and twenty faces. The bracketed numbers following the names $\{m, n\}$  of the figures are called *Schläfli symbols* and relate to topology in the following way. The first number  $m$  refers to the number of edges that meet at a vertex while  $n$  is the number of edges that bound a face. Note that the tetrahedron is termed “self dual” while the cube and octahedron and dodecahedron and icosahedron are respectively dual pairs; their symbols have  $m$  and  $n$  interchanged. Duality is the mathematical property of higher dimensional geometries that states that linear elements of dimension 0 are dual to elements of dimension  $d - 1$  where  $d$  is the number of dimensions of the space under consideration. *E.g.*, in the two dimensional plane,  $d = 2$ , points,  $d - 2 = 0$ , are dual to lines,  $d - 1 = 1$ , while in three dimensional space,  $d = 3$ , points,  $d - 3 = 0$ , are dual to planes,  $d - 1 = 2$ . The line,  $d - 2 = 1$ , is self dual in three dimensional space as it may be defined either on a pair of points or on a pair of planes. Such *synthetic* geometric relations will be pursued no further in this course.

### 2.9.3 Cube, Tetrahedron and Octahedron

We begin with the **cube** because its shape and symmetries are most familiar and conform quite perfectly to the three orthogonal Cartesian axes. Fig. 9 shows front and right side views of an origin centred cube, with edges of length 2, and a first and second auxiliary view constructed from the front view projection.

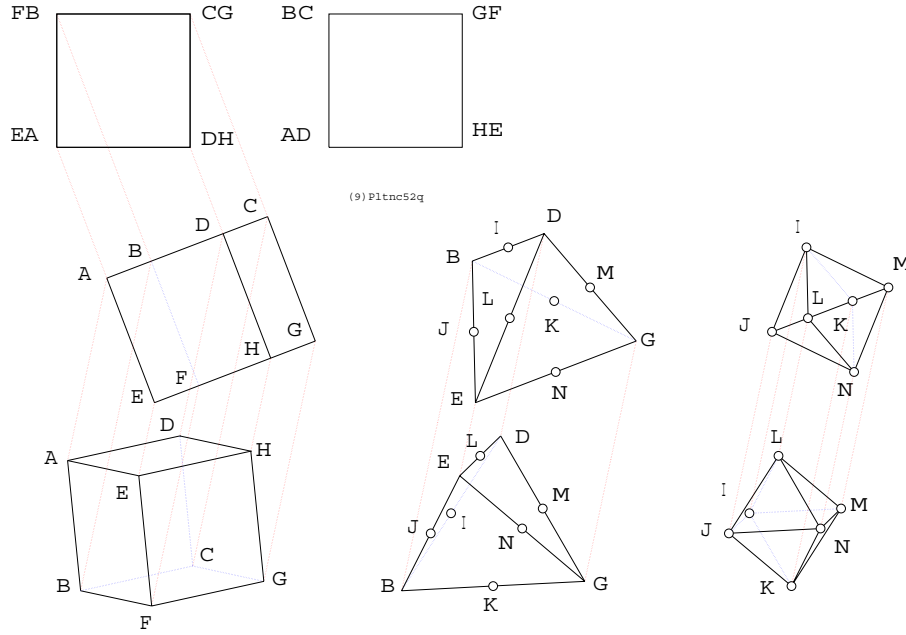


Figure 9: Tetrahedron and Octahedron from the Double Unit Cube

Corner coordinates are

$$A(-1, -1, -1), B(-1, -1, 1), C(1, -1, 1), D(1, -1, -1),$$

$$E(-1, 1, -1), F(-1, 1, 1), G(1, 1, 1), H(1, 1, -1)$$

Note that the angle between intersecting edge pairs, plane pairs and edge-plane pairs is, uniformly,  $\pi/2$ . As an exercise try to identify all planes and lines of symmetry with respect to the cube. Such a plane divides the cube into congruent halves while a point view of a line of symmetry reveals that point at the centre of the cube projected as a regular polygon; either a square or a hexagon.

The **tetrahedron** can be built with six edges formed by face diagonals on the cube. Once, say,  $BD$  has been chosen then  $EG$  is defined as its skew, or non-intersecting, partner.  $BE, BG, DE, DG$  provide the vertex pairs on the remaining four edges. Every face is an equilateral triangle with sides of length  $2\sqrt{2}$ . Since the vertex coordinates are tabulated above the angle between a pair of typical face planes can be obtained with Eq. 8 using the following point position vectors.

$$\cos(\pi - \phi) = \mathbf{m} \cdot \mathbf{n}, \quad \mathbf{m} = \frac{(\mathbf{e} - \mathbf{b}) \times (\mathbf{d} - \mathbf{b})}{\|\mathbf{e} - \mathbf{b}\| \|\mathbf{d} - \mathbf{b}\|}, \quad \mathbf{n} = \frac{(\mathbf{d} - \mathbf{b}) \times (\mathbf{g} - \mathbf{b})}{\|\mathbf{d} - \mathbf{b}\| \|\mathbf{g} - \mathbf{b}\|} = -\frac{1}{3} \quad (9)$$

The **octahedron** can be built with six vertices on the respective midpoints of the six edges of the tetrahedron or on the midpoints of the six cube faces. These points are tabulated below.

$$I(0, -1, 0), J(-1, 0, 0), K(0, 0, 1), L(0, 0, -1), M(1, 0, 0), N(0, 1, 0)$$

Notice how duality between cube and octahedron comes into play. The transformation from one to the other, while retaining all essential symmetries, is accomplished by interchanging points (vertices) with planes (faces). With the six vertex coordinates, an equation similar to Eq. 9 and position vectors  $\mathbf{i}$ ,  $\mathbf{j}$ ,  $\mathbf{l}$  and  $\mathbf{m}$  instead of  $\mathbf{e}$ ,  $\mathbf{b}$ ,  $\mathbf{d}$  and  $\mathbf{g}$  it is easy to show that  $\cos(\pi - \phi) = -\frac{2}{3}$ .

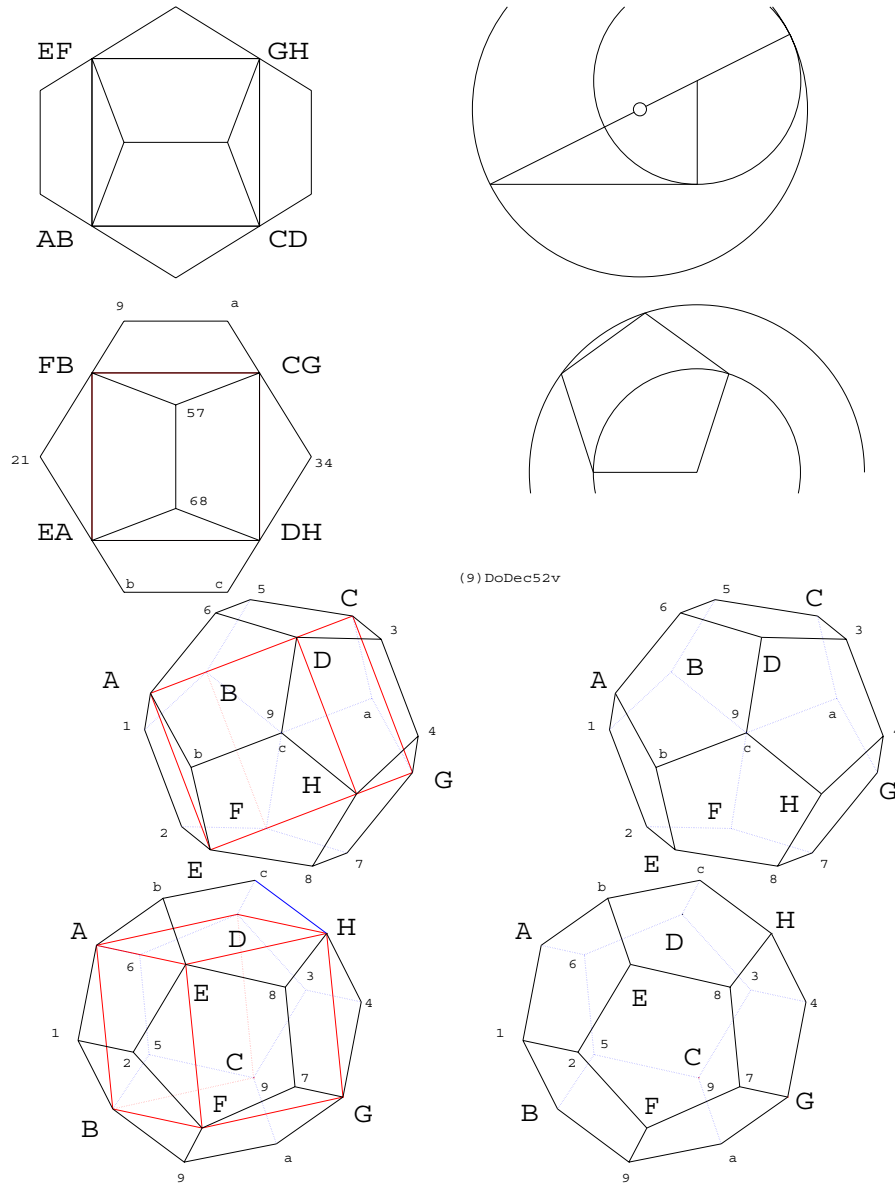


Figure 10: “Golden Ratio”, Pentagon and Dodecahedron

The **dodecahedron** can be built on the cube as well. This time the construction makes use of the twelve cube edges which assume the rôle of diagonals of the twelve regular pentagonal faces of the dodecahedron. Examine Fig. 10. At upper right the construction of a regular



pentagon is presented. Taking a side length of unity, the diagonal length is given by the so called “golden ratio” which is defined as half of the hypotenuse, extended by one unit length, of a right triangle with sides of one and two units length. In this case the construction has been scaled so that the pentagonal diagonal length is 2 so the pentagon side is  $2p = \sqrt{5} - 1$ . With a little plane trigonometry, the twelve “off cube corner” dodecahedral vertices determined as shown below.

$$1(-1 - p, -p, 0), 2(-1 - p, p, 0), 3(1 + p, -p, 0), 4(1 + p, p, 0), 5(0, -1 - p, p), 6(0, -1 - p, -p)$$

$$7(0, 1 + p, p), 8(0, 1 + p, -p), 9(-p, 0, 1 + p), a(p, 0, 1 + p), b(-p, 0, -1 - p), c(p, 0, -1 - p)$$

Eq. 9 demonstrates how to find the angle between plane segments sharing a common line segment.

The **icosahedron** is built with the duality principle. The centre points of the twelve pentagons on the dodecahedron become the vertices of the icosahedron. Fig. 11 shows these vertices labelled with the two letters of the cube edge segment end points that define a particular pentagonal face.

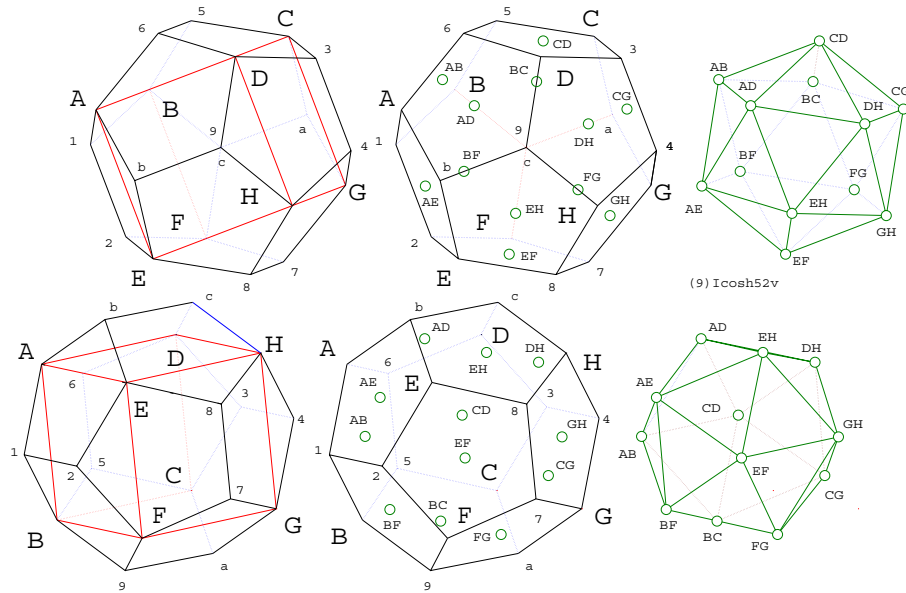


Figure 11: Icosahedron via Dodecahedron and Cube

To obtain any of these points, say,  $BF$ , the origin at the cube centre is projected normally onto the plane segment on points  $BF9$ . Eq. 5 may be used directly to find  $BF$ . Alternately one may use points  $BF9$ , three on the pentagon in question, to find the coefficients of the plane’s equation

$$P_0 + P_1x + P_2y + P_3z = 0$$

find the parameter  $t$  as

$$t = \frac{P_0}{P_1^2 + P_2^2 + P_3^2}$$

and get the coordinates of  $BF$  as

$$x = P_1 t, \quad y = P_2 t, \quad z = P_3 t$$

The centre points of the pentagonal faces of the dodecahedron built on cube edges of length 2, *i.e.*, the icosahedron's vertices, are listed below.

$$AB(q, r, 0), \quad CD(-q, r, 0), \quad AD(0, q, r), \quad EH(0, -q, r), \quad EF(q, -r, 0), \quad GH(-q, -r, 0)$$

$$BC(0, q, -r), \quad FG(0, -q, -r), \quad DH(-r, 0, q), \quad CG(-r, 0, -q), \quad AE(r, 0, q), \quad BF(r, 0, -q)$$

where

$$q = \frac{2}{\sqrt{5} - 5}, \quad r = \frac{\sqrt{5} + 1}{\sqrt{5} - 5}$$

### 3 Geometry in Mechanics

Six topics are introduced here to reveal the intimate connection between engineering mechanics and geometric thinking. To begin with, three examples, pertaining to statics and kinematics, as encountered in virtually every first course in mechanics, are treated from a geometric point of view. Then three corresponding examples, pertaining to spatial statics and kinematics, are addressed. The idea here is not so much to promote graphical rather than equation-based problem solving but to lead one to appreciate the underlying geometry that emerges from the principal invariants of statics and kinematics of rigid bodies.

#### 3.1 Velocities of a Planar Body

Consider the translational instantaneous velocities of points on a planar rigid body and how these relate to the instant centre (point) of zero velocity that lies on the body, or some extension thereof, and the instantaneous angular velocity. Examine Fig. 12. At any instant an arbitrary point fixed to a rigid body  $A$  may experience (or have assigned to it) an arbitrary velocity  $V_A$ . Another point  $B$  may, at this instant, experience any velocity  $V_B$  so long as the component of  $\mathbf{v}_B$  parallel to the line segment  $AB$  is identical to that component of  $\mathbf{v}_A$ .

$$\mathbf{v}_{A(=)} = \mathbf{v}_{B(=)} \quad (10)$$

The relative velocity of  $B$  with respect to  $A$  is

$$\mathbf{v}_{B/A} = \mathbf{v}_B - \mathbf{v}_A = \boldsymbol{\omega} \times \mathbf{r}_{B/A}, \quad \mathbf{r}_{B/A} = \mathbf{b} - \mathbf{a} \quad (11)$$

where  $\boldsymbol{\omega}$  is the instantaneous angular velocity. Lines on  $A$  and  $B$  constructed normal to  $\mathbf{v}_A$  and  $\mathbf{v}_B$ , respectively, intersect on point  $C = C_I$ , the instant centre. Note that  $C_I$  is deemed to be on the rigid body. If it happens to fall outside some arbitrary outline that is drawn, one may imagine the body to extend beyond, in fact indefinitely, like some great sheet of ice in which the finite body is frozen; its motion being taken as the motion of the solid ice sheet. Now the velocity of *any* point  $P$  can be described as a rotation about  $C$  or

$$\mathbf{v}_P = \boldsymbol{\omega} \times \mathbf{r}_{P/C} \quad (12)$$

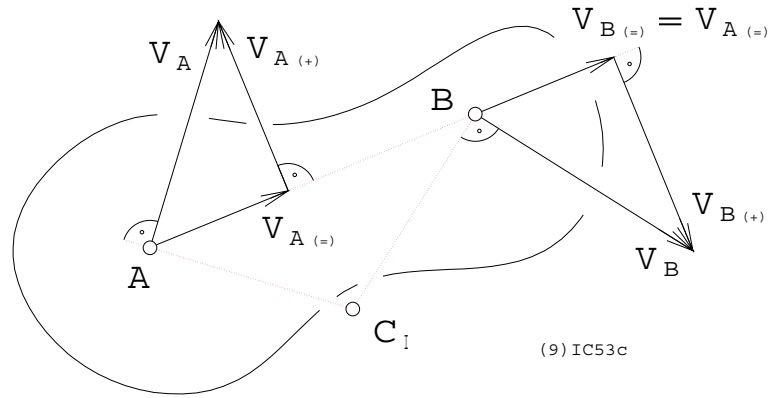


Figure 12: Instant Centre of Zero Velocity

### 3.2 Displacement of a Planar Body

Consider a finite displacement, *i.e.*, two distinct poses of a planar rigid body as shown in Fig. 13, and its relation to a point on the body, or its extension, that remains fixed. Again the rigid body introduced in Fig. 12 is shown with the same points  $A$  and  $B$ . This time however a second image on the right describes a displacement that has occurred. Arrows depict the translation vectors of the two points as if they had moved in straight lines. Right bisectors of the vectors intersect on  $P = P_D$ , called the displacement pole. Now all points on the rigid body can be seen to have moved on equiangular circular arcs centred on  $P$ . If the body undergoes a pure translation then the pole is at an indefinitely great distance normal to the pair of (now) parallel vectors. The instant centre is useful in analyzing motion between bodies in contact that roll without slipping. Such situations include cases involving wheels, gears and cams.

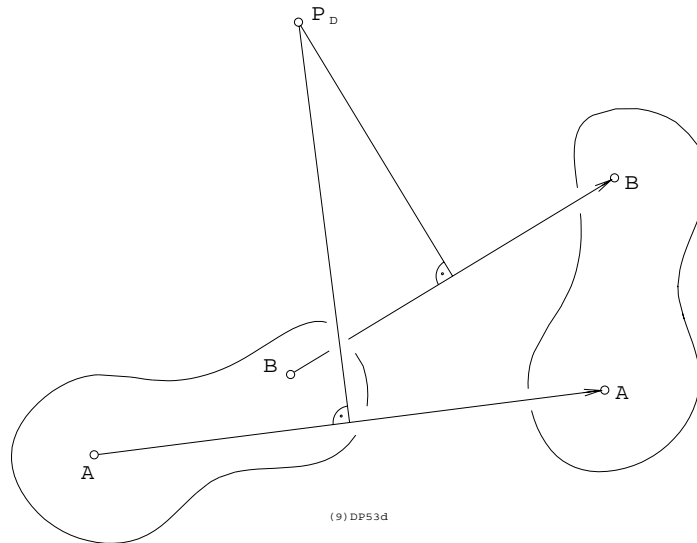


Figure 13: Displacement Pole

### 3.3 Analysis of Planar Pin Jointed Trusses

In every statics course the student is introduced to planar trusses composed of members connected by pins or hinges. When subjected only to concentrated loads at these points all members sustain pure axial force, *i.e.*, tension, compression or null. There are important reasons to study such structures even though they are not often built nowadays.

- Given a system of such loads and members the forces in individual members are easy to determine.
- The configuration bears considerable resemblance to finite element analytic meshes thus providing a natural introduction to more advanced and very popular variants of FEM.
- When compared with more commonly encountered, modern rigid member joint designs, *e.g.*, welded, pin joint analysis predictions always dictate the most conservative design and thereby provide a fast check and some control on more elaborate design analysis procedure.

Text books expose “the method of joints” and “the method of sections”. These concentrate on analyzing a few selected members in the truss. In contrast, “The Maxwell diagram”, making use of an elegant node-branch graph transformation called “Bow’s notation”, is a rapid graphical method that provides a complete analysis and avoids confusion, caused by placing arrows to denote tension *-vs-* compression, by making all force vectors bidirectional and identifying the axial load type with a consistent from-to, left-right convention that

is easily learned and unerringly applied. This method is best understood via an example. Consider Fig. 14.

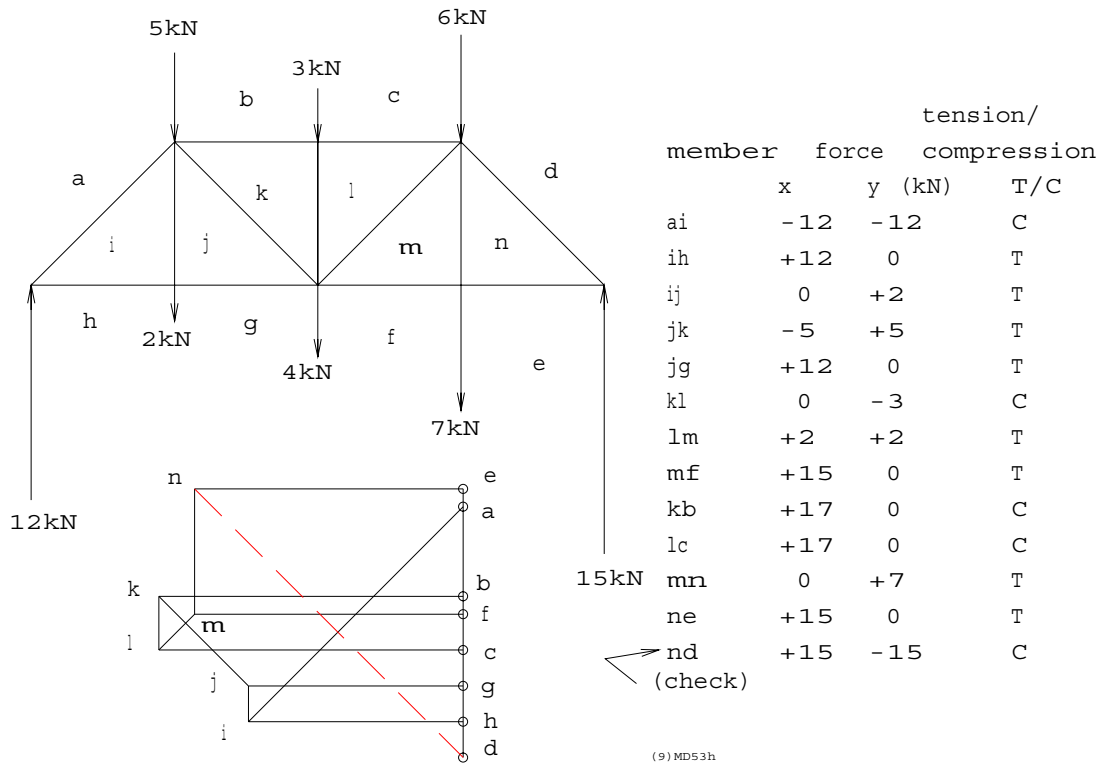


Figure 14: Pin Joint Truss Analysis via Maxwell Diagram

A six right triangular panel truss with 1 : 1 sides is shown to be loaded with six vertically downward concentrated (line) loads as specified. First the reactions of 12kN and 15kN are established in the conventional way by applying force and moment equilibrium. Although there is a geometric way, called “funicular polygon”, to do this, its explanation does not seem worthwhile. Analysis proceeds as follows.

1. Bow’s notation is invoked, *i.e.*, rather than labelling every joint, each side of every line that represents a member or external force is labelled, starting with a clockwise circuit to label the six imposed loads and two upward reactions. *E.g.*, the 5kN force is labelled *ab* while the right hand, upward 15kN reaction is called *de*. All the interior regions of triangular panels are labelled as well.
2. A “degenerate” (zero area) force vector polygon addition of the external loads and reactions is carried out in the alphabetical, clockwise sequence. It appears beneath the truss. This polygon consists of vectors that lie in a single vertical line since all external forces are vertical. Beginning to end labelling on the polygon reflects the clockwise sequence. *E.g.*,  $a \rightarrow b$  is plotted proportional in length to 5kN and the sense

is downward. Similarly the sequence  $d \rightarrow e$  is upward and proportional in length to 15kN.

3. Now the six points represented by  $i$  to  $n$  are located. This is done by taking each pin as a rigid body in static equilibrium under influence of the axial force members, external loads and/or reactions radiating from it. *E.g.*, the pin at the left hand reaction is called  $aih$  (or either of the other two possible sequences of clockwise labelling around that pin). The point  $i$  is located on the intersection of a line on  $a$  and parallel to the member labelled  $ai$  on the drawing of the truss and another on  $h$  and parallel to the member on the truss drawing between labels  $i$  and  $h$ .
4. The forces in  $ai$  and  $ih$  are immediately available as measured as lengths on the force polygon. To determine whether the loading is tensile or compressive we carry out a thought experiment by “standing” on the pin  $aih$  and making the following observation. Look at  $ai$  on the truss then examine the sense of the sequence  $a \rightarrow i$ . It bears *toward* the observer. Therefore the load in  $ai$  must be compressive (C) because, for  $ai$  to “push” the observer looking at it “backwards” that member must be under compression.
5. Maintaining this initial observer position, look at  $ih$  and examine the sense of the sequence on the force polygon  $i \rightarrow h$  that is “eastward”, away from the observer. Therefore this is a tensile member under the given system of loads.
6. The procedure is repeated, with the observer at, say, pin  $jghi$  as labelled in clockwise circulation. Note that at each step only pins radiating two members of unknown axial force may be addressed.
7. Member “names” are tabulated together with the Cartesian force components they sustain. The sense (+/–) depends on where the observer stood. *E.g.*, when tabulating  $lm$  the observer was on pin  $lmfgjk$ , not  $mlcdn$ , because  $lm$  is clockwise with respect to the first, not second sequence of labels that identifies a pin. Notice that if the observer goes to the opposite pin on a member the direction of the observed force reverses but the sense of toward/away remains.
8. Finally, examine  $n \rightarrow d$ , represented by a broken line on the force polygon. The Maxwell diagram (the plot of the force polygon containing all internal labels on the truss) was complete before the observer stood on pin  $den$ . Therefore to determine force  $nd$  one needs only to join these two existing points and measure the interval. Generally, if errors occurred, the direction of the broken line would deviate from that of the member  $nd$  on the truss drawing.

### 3.4 Velocities of a Spatial Body

“Twist” is the spatial equivalent of angular velocity about the instant centre in the plane. It is composed of an instantaneous axis  $XY$  and lead and angular velocities of a rigid body like that shown in Fig. 15.

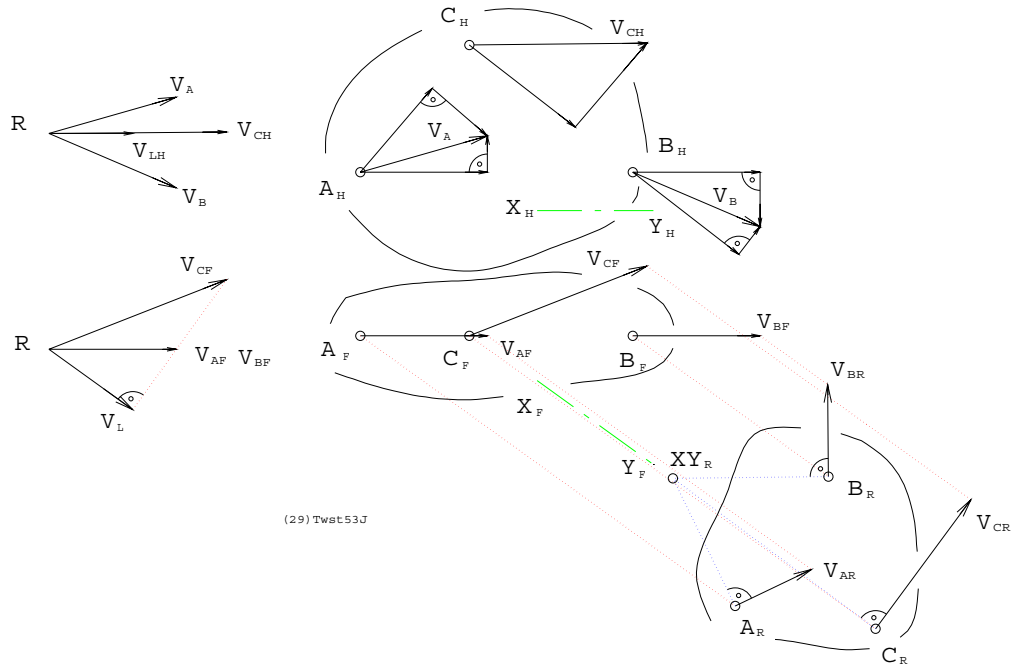


Figure 15: Instantaneous Twist

Three points  $A, B, C$  are shown.  $A$  is assigned an arbitrary instantaneous velocity  $V_A$ . Then  $B$  may have any velocity  $V_B$  as long as its component parallel to line  $AB$  is the same as that of  $V_A$ . Point  $C$  is constrained to sustain velocity  $V_C$  such that the component of  $V_C$  parallel to line  $BC$  is the same as that of  $V_B$ . Similarly, components of  $V_A$  and  $V_C$  along  $AC$  are identical. The only component of  $V_C$  that may be freely imposed is that normal to plane  $ABC$ . Notice that  $V_A$  and  $V_B$  were chosen to be coplanar. This is of course not necessary but it simplifies construction of the lead velocity vector  $V_L$ . To do this, top and front views of all three velocity vectors are plotted to scale, radiating from common point  $R$ . Note that the tips of the three velocity vectors  $V_{AF}$ ,  $V_{BF}$  and  $V_{CF}$  fall in a planar line view. That was the reason for the coplanar velocity simplification; to save an auxiliary construction. Now the lead velocity  $V_L$  appears normal to this planar edge. If the points  $A, B, C$  are projected to a view where  $V_L$  would appear as a point then velocity components  $V_{AR}$ ,  $V_{BR}$  and  $V_{CR}$  are normal to the twist axis whose end view  $XY_R$  is on normals to  $V_{AR}$ ,  $V_{BR}$  and  $V_{CR}$  drawn respectively on  $A_R, B_R, C_R$ . Angular velocity of twist  $\omega$  can be seen to be righthanded and its magnitude is determined by dividing, say,  $V_{AR}$  by the length of the normal  $XY_R \rightarrow A_R$ .



### 3.5 Displacement of a Spatial Body

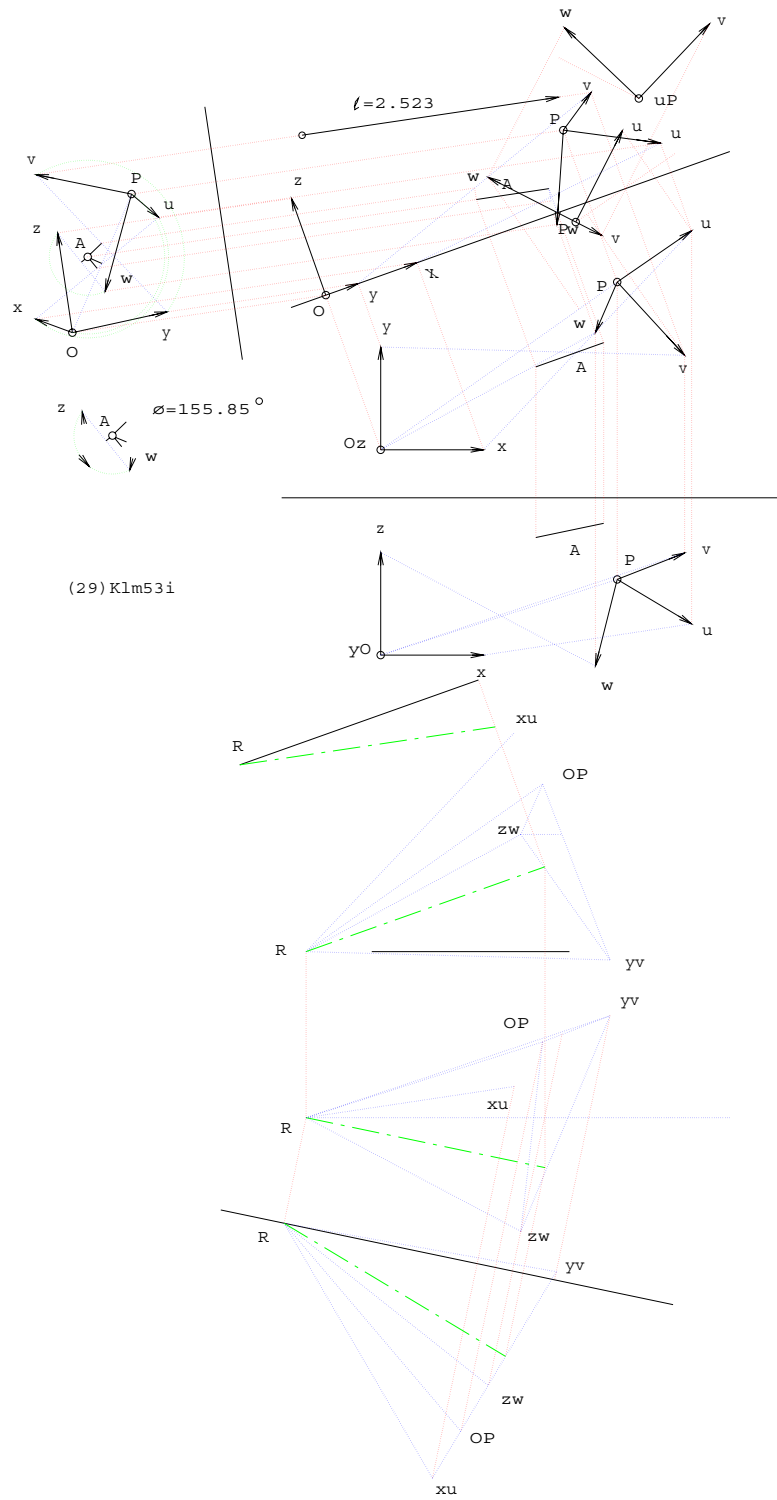


Figure 16: Finite Screw Displacement

Screw axis, rotational angle and translational lead, given two views of a unit Cartesian axis triad in an original or “home” pose and one finitely displaced, are constructed as shown in Fig. 16. These three displacement parameters correspond to the two, *viz.*, displacement pole and rotation angle, encountered in two dimensional motion and described in Fig. 13. They are constructed in the following way.

1. Notice the original pose defined on origin  $O$  and the tips of the unit axes labelled  $x, y, z$  respectively. In the corresponding displaced pose these become  $P, u, v, w$ .
2. Now consider the four displacement vectors  $O \rightarrow P, x \rightarrow u, y \rightarrow v, z \rightarrow w$ . If these are plotted, below, in two similar top and front views and radiating from a common point  $R$  we see these vector tips labelled as  $OP, xu, yv$  and  $zw$ .
3. Then examine the triangular plane segment  $yv \ zw \ OP$ . An edge or line view was constructed. It is noted with satisfaction that  $xu$  also falls in the plane. A normal to the plane extended from  $R$  is shown as a dash-dotted centre line. All four point displacement vectors project a common component length onto this direction. The length of this normal is the lead of the screw.
4. If an end or point view of this normal direction is constructed, only those components of the displacement vectors that are normal to the screw axis project on it. They can be accounted for by rotation about the axis.
5. The point view construction is accomplished with the line segment labelled  $A$  that is on the axis. But we don't yet know where it is located. But any line parallel to the axis will do to obtain a projection in which the axis appears as a point.
6. Once this has been done, right bisectors of the displacement vector projections are taken. These intersect on the point view of  $A$  which can be returned by projection to the original reference frame of top and front view.
7. Finally each displacement vector in the axial point view projection subtends a chord of a circular arc of rotation about the screw axis. Note that this has been measured as  $\phi = 155.85^\circ$  in this example while the lead is  $l = 2.523$ .

### 3.6 Resultant Wrench

Imagine the most compact representation of a three dimensional loading system that includes concentrated forces represented by vectors  $\mathbf{F}_i, \ i = 1 \dots m$ , each acting on a line located by the position vector  $\mathbf{r}_i$  of an arbitrary point on it. In addition, the system contains a set of torques represented by the couple vectors  $\mathbf{C}_j, \ j = 1 \dots n$ . This acts on a rigid body and if we are concerned only with how the body interacts with others to which it is connected, not with internal shear and bending, then the system can be combined and represented by a single resultant force  $\mathbf{R}$  and a single resultant torque  $\mathbf{T}$ . By assuming  $\mathbf{R}$  acts along a line

on the origin  $O$  we obtain

$$\mathbf{R} = \sum_{i=1}^m \mathbf{F}_i, \quad \mathbf{T} = \sum_{i=1}^m \mathbf{r}_i \times \mathbf{F}_i + \sum_{j=1}^n \mathbf{C}_j \quad (13)$$

A typical situation is shown in Fig. 17 where on the left we see top, front and right side views of  $\mathbf{R}$  and  $\mathbf{T}$ .

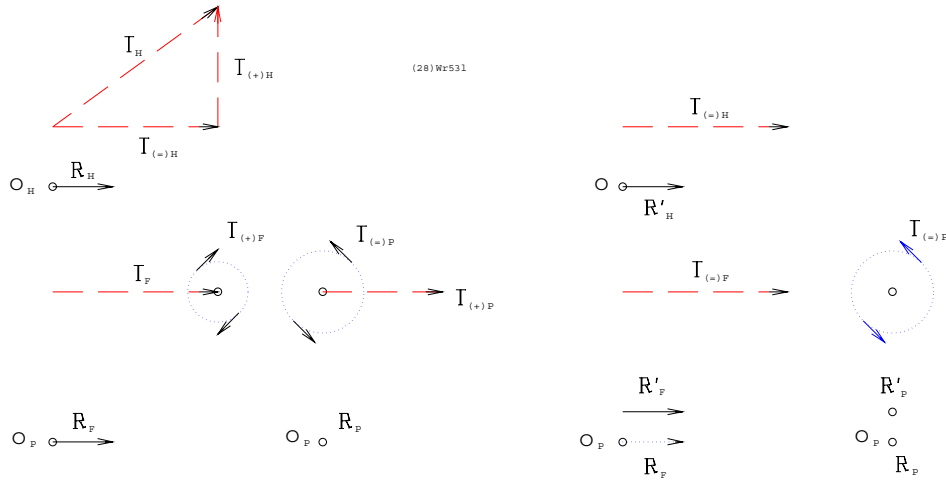


Figure 17: Resultant Wrench

There is no loss of generality by choosing a Cartesian frame so that  $\mathbf{R}$  is along the  $x$ -axis and  $\mathbf{T}$  is normal to  $z$ . Notice that  $\mathbf{T}$  has been decomposed into  $\mathbf{T}_{(=)}$  and  $\mathbf{T}_{(+)}$ , respectively parallel and normal to  $\mathbf{R}$ . Notice that  $\mathbf{T}$  and its components are shown redundantly as broken line vectors and their equivalent couples. As long as direction is maintained, it does not matter where these are placed on the rigid body (not shown). Since a force can generate any moment vector in the direction normal to the force, the most compact representation of the loading system is achieved by translating  $\mathbf{R}$  from the origin so as to generate  $\mathbf{T}_{(+)}$  about  $O$  and the system is reduced to that shown in the three views on the right,  $\mathbf{R}' + \mathbf{T}_{(=)}$ . Let us call this the “resultant wrench”, If  $\mathbf{T}_{(=)}$  is in the same sense as  $\mathbf{R}'$  this is a right handed screw. There exists a kinetostatic duality between twist and wrench wherein the line of  $\mathbf{R}'$  assumes the rôle of axis,  $\mathbf{T}_{(=)}$  assumes that of lead velocity  $V_L$  and the moment field generated by  $\mathbf{R}'$  is the dual counterpart of the rotational velocity field caused by  $\omega$  represented at the three discrete points  $A, B, C$  as  $V_{AR}, V_{BR}, V_{CR}$  shown in Fig. 15.

## 4 Symmetry and Solid Modelling

This section touches first on conceptual representation (RC) of three dimensional objects. RC includes three types. Their names are quite self-descriptive. They are “wire frame”, “B-rep” (short for *boundary representation*), solid primitives (ideal objects, like sphere, cylinder, block and wedge) that can be distorted and assembled in Boolean combination to assume a remarkably large variety of, if not all, possible objects. Then comes storage representation (RS) or how objects are described in a CAD database. RC types map approximately to corresponding RS types. A set of spatial curve (including straight line) segment descriptors, related by a connectivity list, is suited to wire frame concept. Biparametric surface patches, appropriately subdivided into various sizes of triangular or quadrilateral facets, suits the B-rep concept. The “octree” idea makes it easy to efficiently store and visually display a collection of distorted solid primitives. An octree begins by dividing a cube of Cartesian space into eight identical octant cubes. If an octant is entirely full or devoid of solid it is tagged with “1” or “0”, respectively. If an octant is neither entirely full or empty, it is tagged with “X”. All “X” octants at a given tree level are further subdivided into octants at the next level of finer “grain”. Subdivision stops when the finest voxel (volumetric cell) spans no more than a pixel (picture cell; on the screen, *e.g.*), when displayed. Parametric curves and surfaces will be elaborated somewhat in section 6. Topics like clipping, windowing, hidden feature removal, and shading and shadowing of various texture, reflectivity and transparency under one or more sources of illumination are more in the realm of computer graphics, beyond the scope of this introduction. Realistic representation of objects by means of perspective projection will be briefly described next however.

### 4.1 Perspective

“Perspective” is the common name for a central projection on a point  $P$  as shown as a pictorial in Fig. 18 and as a top and front (v/p) pair in Fig. 19.

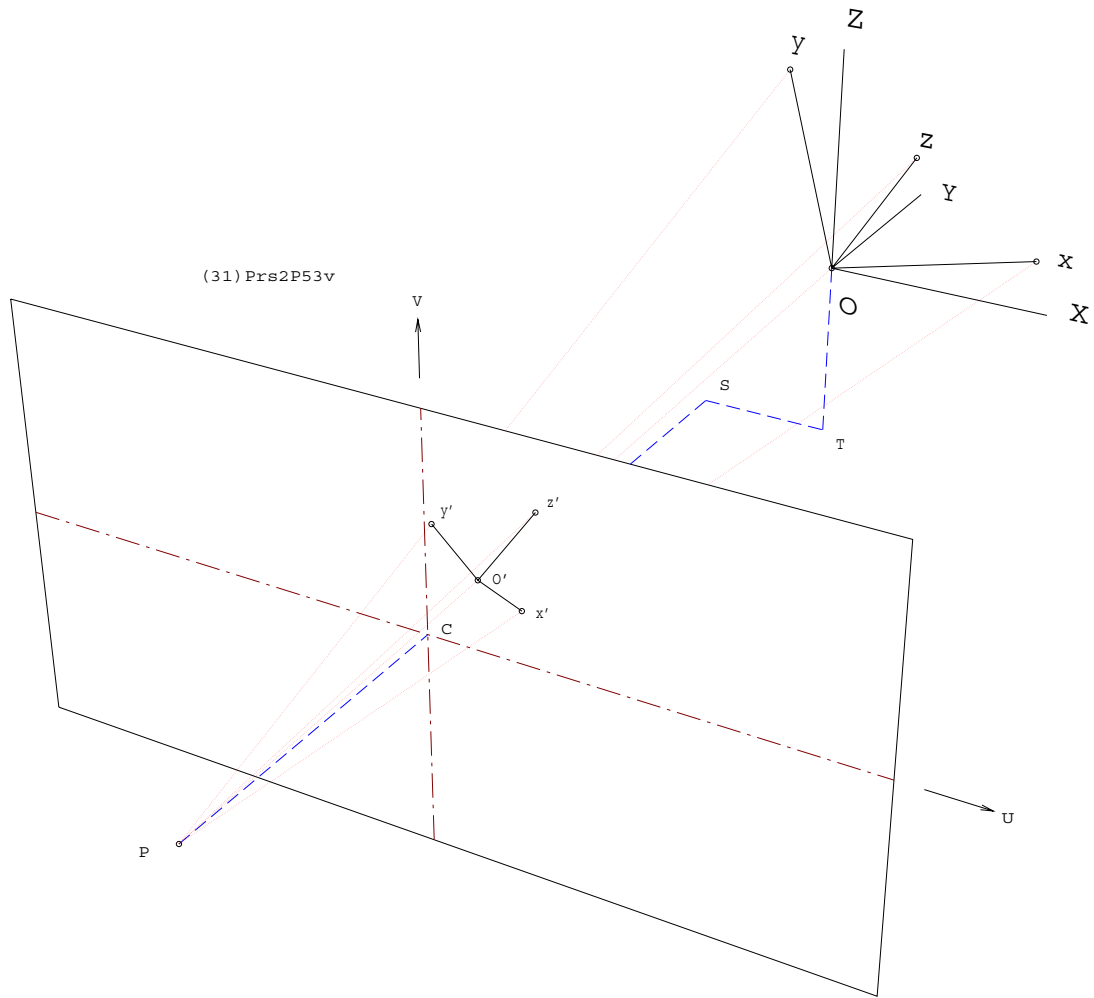


Figure 18: Perspective Projection Pictorial

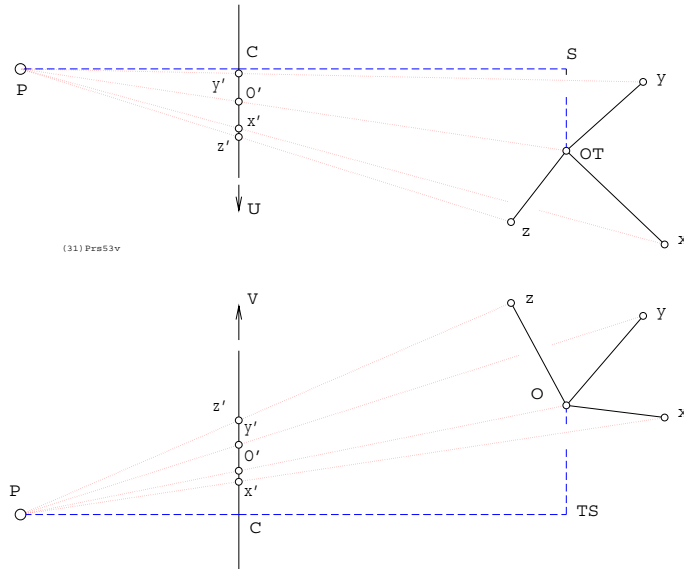


Figure 19: Perspective Projection in Two Views

Here, features of an object (not shown) is to be mapped from a so called “object natural” Cartesian frame  $Oxyz$  to a picture plane Cartesian frame  $CUV$ . This is done by connecting all points of interest in  $Oxyz$  to an “observer” point  $P$ . This may be thought of as the viewer’s eyeball. Notice that  $PC$  is the normal from  $P$  to the origin  $C$  of the planar frame  $CUV$ . The Cartesian frame  $OXYZ$  is a pure translation of  $CUSV$ , the frame in which object point data are expressed, by  $(ST, CS, TO)$  and the frame  $Oxyz$  is displaced from  $OXYZ$  by a right hand rotation through some specified angle  $\phi$  about a specified axis from  $O$  to any point with global coordinates on meridian east longitude  $\mu$  and north latitude  $\lambda$ . Imagine the prime meridian on  $XZ$  and  $Z$  on the north pole. In the example shown the four points  $Oxyz$  will appear as images  $O', x', y', z'$  on the picture plane. These are the piercing points of lines  $PO, Px, Py, Pz$ . The translational offset distances of  $OXYZ$  from  $CUSV$  are easy to see as are the coordinates  $P(0, CP, 0)$ . The rotation that transforms points, expressed in  $Oxyz$ , to  $OXYZ$  requires some explanation.

## 4.2 Rotation

There are many ways to describe points in a rotated frame. Here, the notion of rotation about a specific fixed axis, as mentioned above, will be used. The illustrations show distances

$$PC = 16, \quad ST = 6, \quad CS = 24, \quad TO = 10$$

and angles

$$\phi = \pi/3, \quad \mu = \pi/6, \quad \lambda = \pi/4$$

It is not hard to see that the direction cosines of the specified rotation axis with respect to  $OXYZ$  are

$$\cos \alpha = \cos \lambda \cos \mu, \quad \cos \beta = \cos \lambda \sin \mu, \quad \cos \gamma = \sin \lambda$$

Elements of the rotation matrix that premultiplies a point position vector, expressed in  $Oxyz$ , to transform its Cartesian coordinates to those of  $OXYZ$ , can be written as the so called Euler vector.

$$\begin{bmatrix} c_0 \\ c_1 \\ c_2 \\ c_3 \end{bmatrix} = \begin{bmatrix} \cos \alpha \\ \cos \alpha \sin \beta \\ \cos \alpha \sin \beta \sin \gamma \\ \cos \alpha \sin \beta \cos \gamma \end{bmatrix}$$

The rotation matrix takes the following form.

$$\mathbf{R} = \begin{bmatrix} c_0^2 + c_1^2 - c_2^2 - c_3^2 & 2(c_1c_2 - c_0c_3) & 2(c_1c_3 + c_0c_2) \\ 2(c_2c_1 + c_0c_3) & c_0^2 - c_1^2 + c_2^2 - c_3^2 & 2(c_2c_3 - c_0c_1) \\ 2(c_3c_1 - c_0c_2) & 2(c_3c_2 + c_0c_1) & c_0^2 - c_1^2 - c_2^2 + c_3^2 \end{bmatrix} \quad (14)$$

After making the required substitution for angles, the points  $x, y, z$ , *i.e.*, the tips of the axis triad expressed in frame  $Oxyz$  as  $(10, 0, 0)$ ,  $(0, 10, 0)$ ,  $(0, 0, 10)$ , are expressed in frame  $OXYZ$ .

$$x = 10 \begin{bmatrix} \frac{11}{16} \\ \frac{\sqrt{3}}{16} (1 + 4\sqrt{2}) \\ \frac{\sqrt{3}}{8} (1 - \sqrt{2}) \end{bmatrix}, \quad y = \begin{bmatrix} \frac{\sqrt{3}}{16} (1 - 4\sqrt{2}) \\ \frac{9}{16} \\ \frac{1}{8} (1 + 3\sqrt{2}) \end{bmatrix}, \quad z = \begin{bmatrix} \frac{\sqrt{3}}{8} (1 + \sqrt{2}) \\ \frac{1}{8} (1 - 3\sqrt{2}) \\ \frac{3}{4} \end{bmatrix}$$

Numerical evaluation of the elements of  $\mathbf{R}$  and planar coordinates of  $O', x', y', z'$  is suggested as an exercise for the student.

### 4.3 Creation and Manipulation

Here some of the essentials of 3D CAD will be described. Wire frame, B-rep and solid primitive paradigms are illustrated and explained in the context of creation and combination of elementary solid objects. One cannot deal with the entire gamut of CAD capability but a serious attempt to hit some high points is made. There will be no beautifully finished examples of CAD renderings that appear in glossy texts and magazines and intimidate the novice user. Nevertheless it is hoped that the reader will come away with a fairly good idea about how it all works. Note that details of precise commands and procedures to do this or that in any specific CAD system are deliberately omitted.

#### 4.3.1 Boolean Operations

Boolean combinations of existing objects will not be illustrated because the notions are naturally intuitive, therefore readily understood. Rather, these are summarized in the following list.

- Put two (or more) objects together so the resulting object is described by the volume common to either or both. This is called “addition” or “inclusive-ORing”.
- Put two objects together so the result is only the volume common to both. This is “exclusive-ORing”.
- Put objects together so the result is the volume remaining of the member designated “blank” after the volume common with the other, designated “cutter”, is removed. This is called “subtraction” hence, unlike the previous operations, non-commutative. Commutative subtraction, *i.e.*, where only the common volume is removed, so that regions of both “cutter” and “blank” may remain, though feasible, is not a feature available as a standard operation. However most CAD systems are augmented with “macro” or custom programmability so the user may enhance their capacity as needs dictate.

### 4.3.2 Creating and Extruding a Planar Outline

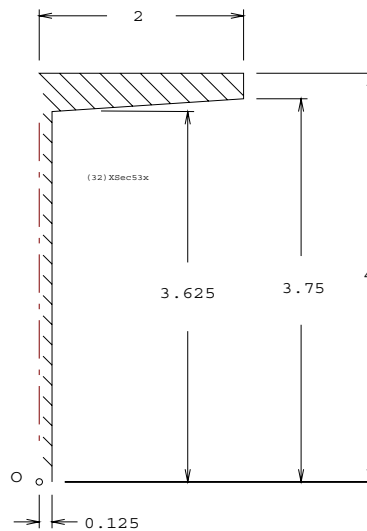


Figure 20: I-Beam Quarter Section

Consider Fig. 20, showing a quarter cross-section of an I-beam. Plotting the five corner points, defined with respect to origin  $O$ , and joining them with straight line segments, produces a “wire” that can be duplicated by reflection or “mirroring” on the vertical axis on  $O$ . Then the composite is mirrored on a horizontal axis on  $O$  to yield the entire “I” outline wire frame. The outline may or may not be designated a “plane” -imagine soap film spanning the closed wire loop. Such a plane appears on the right of Figs. 21 and 22.



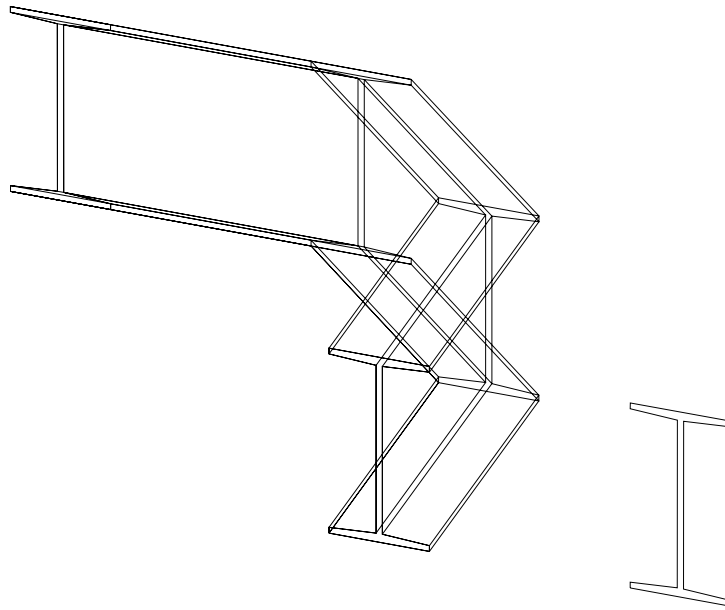


Figure 21: Wire Frame I-Beam Extrusions

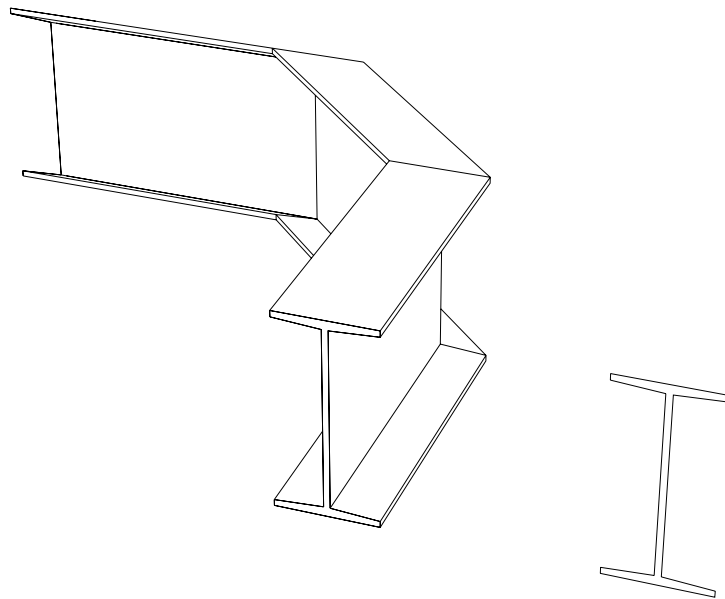


Figure 22: I-Beam Extrusions with Hidden Line Removal

Three points are attached to objects that will be subject to further manipulation, *e.g.*, the point  $O$  and one a unit to the right, horizontally, and a third, a unit perpendicularly “into the paper” on Fig. 20. These are called “handles” and are placed where desired in space when the original object is moved or duplicated. The “extrusion” illustrated in Figs. 21 and

22 was done by establishing points

$$(0, 0, 0), (0, 12, 0), (-8, 20, 0), (-20, 20, 0)$$

with respect to  $O$  before issuing the command that pushed out the section, crab-walked it to the left without changing section orientation and finally smearing it sideways to make the planar outline on the wall at  $y = 20$ . Shading and hidden line removal, Fig. 22, are required to render the image readable since the original wire frame representation, Fig. 21 is highly subject to “Necker” confusion.

### 4.3.3 Slicing and Insertion

Consider a 12-unit long section of the beam described in section 4.3.2. In Fig. 23 the original rectangular piece was duplicated at left.

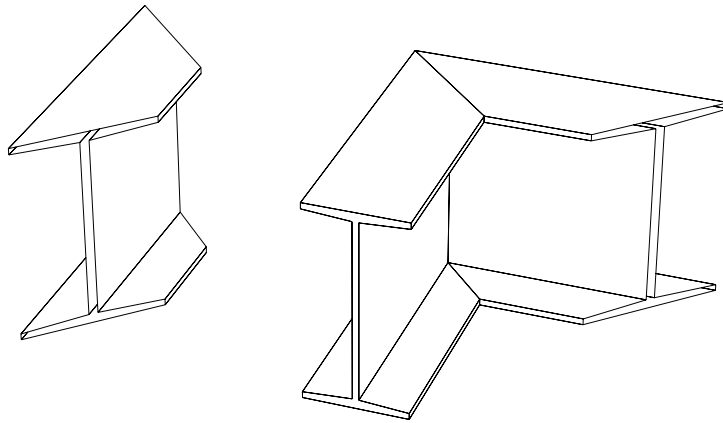


Figure 23: Slicing and Assembling a Corner Joined I-Beam

Then, while maintaining its original length, the duplicate was sliced with a vertical “near” plane striking NE and a “far” plane striking SE. The original piece was cut similarly but only with a SE plane. The handles used to place the double cut piece on the original were selected on extreme corners of the bevelled, near face. A slice is defined by any three points on the cutting plane while a fourth, not on the plane, is on the side where material is to be removed. Notice the “egg shell” (visible internal edges) effect on sections produced by a slice that reveals the B-rep nature of this model. The user must be careful that (infinite) cutting planes do not chop unintended objects. This can be prevented, usually, by “layering” which can place inactive objects out of harm’s way.

### 4.3.4 Sweep and Scale

Examine Figs. 24 and 25.

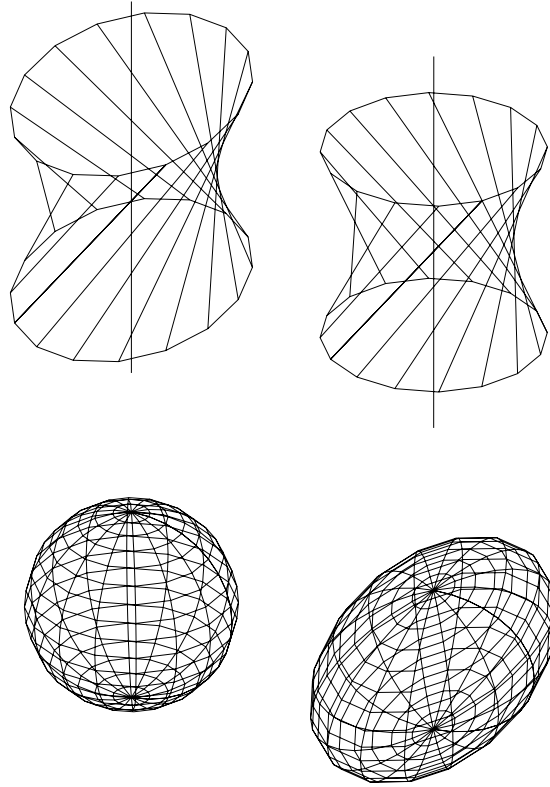


Figure 24: Rescaled Wire Frame Quadrics of revolution

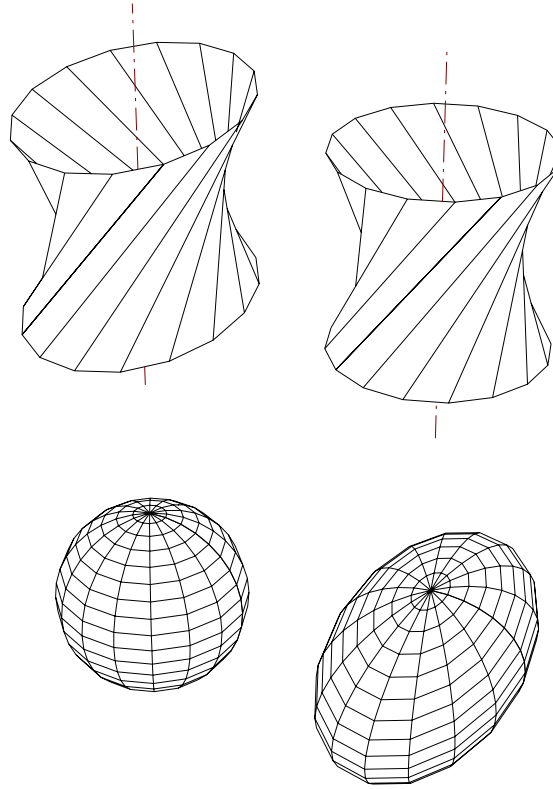


Figure 25: Rescaled Quadrics of Revolution with Hidden Line Removal

First, one perceives how a quadric, a hyperboloid of one sheet, is generated by rotating a line to sweep a  $\pm 4$ -unit right truncation of the surface with respect to its throat centre. This was done by defining a (vertical) axis line on, say,  $(0, 0, -8)$  and  $(0, 0, 8)$ . Then a generator was defined on  $(-3, -3, -4)$  and  $(-3, 3, 4)$ . Designating this second line segment to be an “object” with handles on  $(0, 0, 0)$ ,  $(1, 0, 0)$ ,  $(0, 1, 0)$  the circular sweep command was invoked with two points on the axis, the complete circle designated by an angle of  $360^\circ$  and fairly coarse tessellation of 16 equispaced generators. The shading is poor because of the coarse facets on  $22.5^\circ$  of arc. More serious, adjacent generators are not even nearly parallel so the soap film surface that spans them is severely twisted and the shading algorithm has a hard time making up its mind. The hyperboloid of revolution on the right is the one that was generated. To create a general hyperboloid one may start with the symmetric one and use scaling. The duplicate on the left was scaled in  $x, y, z$  as  $(\times 1, \times 1.5, \times 1)$ , *i.e.*, the elliptical right sections have their major axes in the  $y$ -direction. Next, the lower left figure, another quadric (sphere of radius 4 units) surface, was constructed using the primitive element concept. It was specified by the centre and any point on the surface. Faceting on 16 equi-angular spaced meridians and latitude circles produces much better shading results, in both the spherical and ellipsoidal varieties. That is because circular or elliptical arc quadrilaterals are perfectly approximated by chordal quadrilaterals on the surface vertices in the former case and pretty well in the latter so long as the scaling parameters do not differ widely. The scaling invoked for the sphere to ellipsoid transformation at lower right is  $(\times 1, \times 2, \times 0.75)$ . Consider that even very simple 3D CAD systems support cube, sphere and cone solid primitives and allow

Boolean operations as well as sweeps and slices. Elementary edge hiding and surface shading are available too. Sweep generated surfaces are not restricted to movement of generators in straight line and circular paths. It is thus possible, *e.g.*, to generate a spiral bevel gear tooth surface with an appropriate extrusion trajectory and varying the scale of the generator along this path.

#### 4.3.5 A Solid Modelling Exercise

Consider the transition piece described in Fig. 32.

- Model it first as 30 triangular plane segments in space. This is lengthy, tedious but straight forward. You can do hidden lines and shading on it and examine various points of view, colouring distribution, *etc.*. These capabilities are available in virtually all CAD systems.
- As a challenge, try to remodel the transition piece using the cone of revolution as a solid primitive. These must be scaled to match the four elliptical cone partial “skirts” that fit on the quadrants of the circular duct and have their vertices on the four corners of the rectangular duct. You will require four different scaling factor triplets. You will require three different cutting plane slices for each skirt. Locating handles is easy. All this is a lot of work but if you succeed you will have proven your solid modelling and geometric thinking prowess.

## 5 Intersections

This section deals with intersection of lines and planes with simple quadrics of revolution to show how points on the curve of intersection between such surfaces are obtained. Furthermore it is shown how a structural member of rectangular cross-section is cut to fit obliquely between specified constraining planes.

### 5.1 Line and Sphere

Consider Fig. 26. This shows how to solve a line and sphere intersection problem. The sphere is given in conjugate (v/p)s by centre  $M$  and radius.

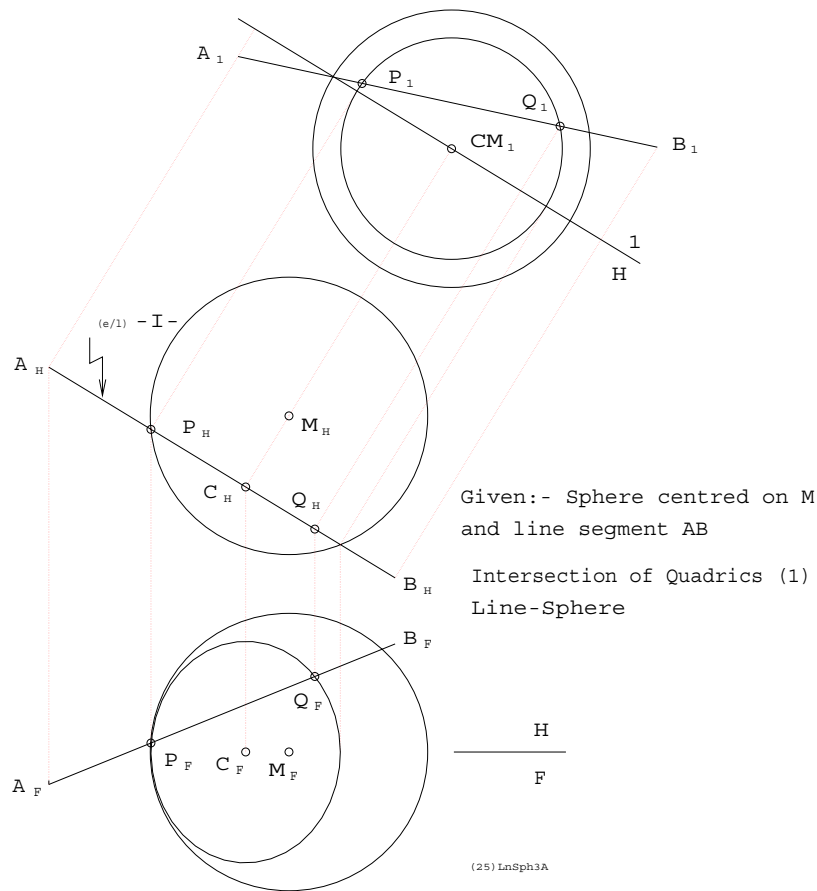


Figure 26: Line and Sphere Intersection

The line segment  $AB$  is given by the coordinates of the two points. One may proceed by taking an auxiliary (v/p) to show (TS) of the vertical plane on  $AB$ . This shows a small circle, centre  $C$ , in that plane. Since  $AB$  is coplanar with the small circle the piercing points of  $AB$

and the sphere are available by inspection as  $P$  and  $Q$  in  $1(v/p)$ . These points are projected into the principal  $(v/p)$ s so one may measure their coordinates. One may also proceed via a direct method construction where the small circle in  $(e/l)$  is noted in  $H(v/p)$ . In  $F(v/p)$  the circle appears as an ellipse. Its major axis is just the diameter of the circle available as the length of the  $(e/l)$  view of the small circle “line” in  $H(v/p)$ . The major axis projects from a vertical “spoke” in the middle of  $(e/l)$  of the small circle. This spoke is in  $(e/p)$ . The minor axis of the ellipse is the  $x$ -span of the small circle, visible in  $H(v/p)$ . The centre  $C$  must have the same  $z$ -coordinate as  $M$ . When the “ellipse” (It’s really just a view of the small circle.) is drawn the intersections  $P$  and  $Q$  are found by inspection.

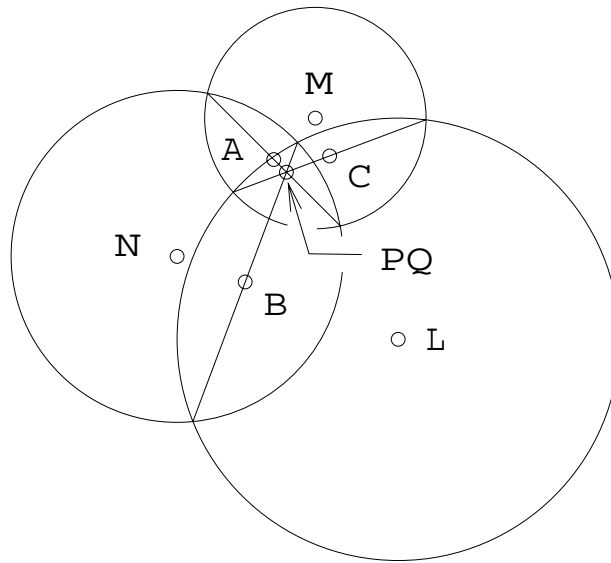
### 5.1.1 Algebra

An equivalent solution via vectors and analytic geometry proceeds as follows. First, recall the parametric equation of a point  $P$  on a line on given points  $A$  and  $B$  and the equation of a sphere of radius  $r$  and centred on  $M(m_x, m_y, m_z)$ .

$$\begin{bmatrix} p_x \\ p_y \\ p_z \end{bmatrix} = \mathbf{p} = \mathbf{a} + t(\mathbf{b} - \mathbf{a}), \quad (p_x - m_x)^2 + (p_y - m_y)^2 + (p_z - m_z)^2 - r^2 = 0 \quad (15)$$

The second equation of Eq. 15, a quadratic in  $t$ , is solved. Then the two piercing points are found with the two values of  $t$  in the first, linear parametric equation of Eq. 15.

## 5.2 Three Spheres



(25) GPSRf5A

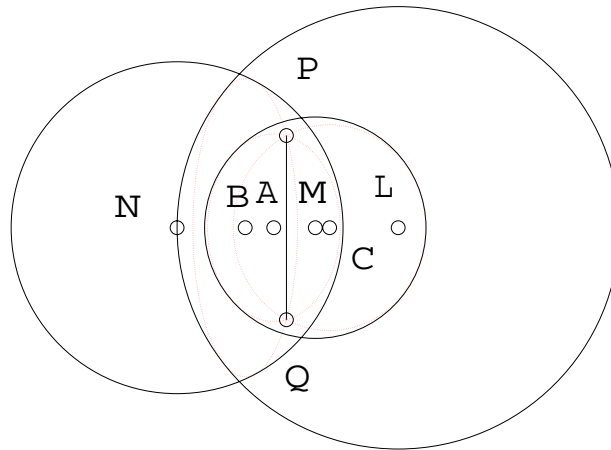


Figure 27: Intersection of Three Spheres

This reflects the principles of satellite global positioning (GPS) Fig. 27 shows how to get the coordinates of a point  $P$  in space from three known stations. This is an example of how sphere/line intersection may be used to advantage in a practical problem. One must appreciate that intersecting spheres do so on circular traces which are planar. All three intersecting circle planes have a common LoX which is used to get  $P$  and  $Q$ . There is no loss in generality if one chooses the principal (v/p)s as (TS) and (e/l), respectively, of the three given sphere centres  $L, M, N$ . This makes the line/sphere intersection much easier than the more general case of Fig. 26, where  $AB$  is *not* (e/p).



### 5.2.1 Algebra

In this case one begins with three spheres with respective radii  $r_i$  and respectively centred on points  $M_i$ . By obtaining the difference between their three equations twice, using different pairs, one obtains two plane equations. These planes each contain the circle of intersection on a pair of spheres. Simultaneous solution of the two linear equations, first with that of principal plane -H-, *i.e.*  $z = 0$ , then with -F-,  $y = 0$ , provides two convenient points to serve as  $A, B$ . Then one proceeds with Eq. 15, using any one of the spheres. With four satellites, four different trios of spheres is available. Solving the problem again with one of the other sets of three will again provide two points located by GPS. However only one of these will be common to between the separate solutions.

### 5.3 Line and Cone

Fig. 28 illustrates the intersection of given line  $AB$  and a cone of revolution whose axis is shown as a frontal-profile line (a horizontal projector). The cone apex is given as point  $X$  and the apex half-angle is  $\tan^{-1} \frac{2}{3}$ .

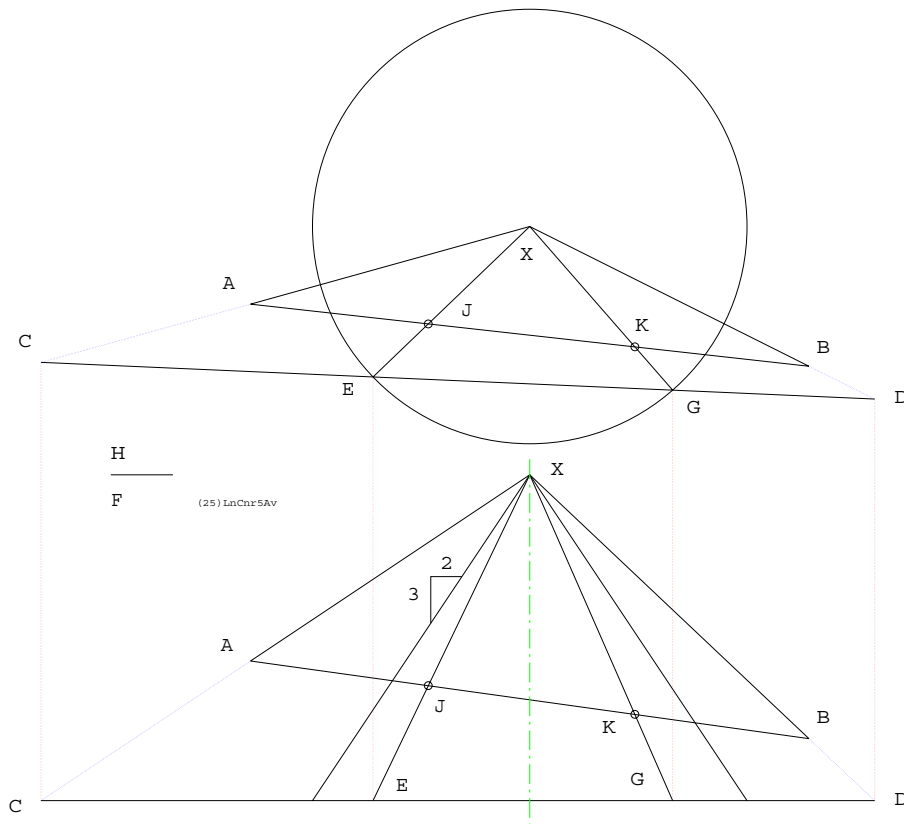


Figure 28: Intersection of Line and Cone

A plane  $ABX$  is constructed and its intersection with some convenient plane (+) to the cone axis is found to cut the cone on a circle.  $XA$  intersects this plane on  $C$  while  $XB$  intersects on  $D$ . The line  $CD$  is coplanar with the circular section of the cone and therefore intersects this circle on  $E$  and  $G$ . Obviously  $XE$  and  $XG$  are on the cone but they are also on the plane  $XAB$ . So  $J$  and  $K$  are simultaneously on the given line  $AB$  and on the cone as well.

### 5.3.1 Algebra

Once again the parametric equation of a point  $P$  on line  $AB$  is used. This time it is paired with the equation of a vertical axis cone to yield the two points of intersection.

$$(p_x - x_x)^2 + (p_y - x_y)^2 - (p_z - x_z)^2 \tan^2 \phi = 0 \quad (16)$$

## 5.4 Cone and Sphere

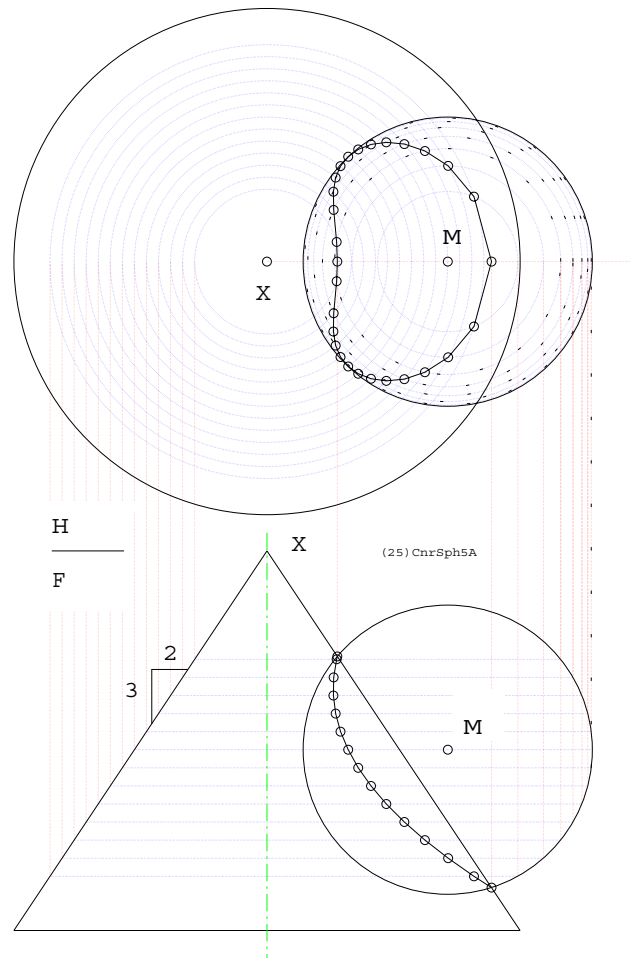


Figure 29: Intersection of Sphere and Cone

Fig. 29 shows the same cone and a sphere centred on  $M$ . The task is to obtain sufficient points on the 4<sup>th</sup> order curve of intersection so that we may map the curve on the surface of the cone and sphere, to be used as, say, structural elements and assembled on the curve. Thirteen horizontal cutting planes at unit spacing are chosen, starting on  $M$  and proceeding up and down. Then the limiting intersecting points, where the frontal meridian circle of the sphere is coplanar with the sphere apex and hence a frontal generator of the cone, are found. Note how the horizontal coplanar circle pairs intersect in H(v/p). That's how 26 of the 28 points on the cone/sphere trace are obtained.

#### 5.4.1 Algebra

This time equations of intersecting coplanar circles, produced by horizontal cutting planes intersecting the sphere and cone, are used.

$$\begin{aligned} (p_x - m_x)^2 + (p_y - m_y)^2 + (p_{zi} - m_z)^2 - r^2 &= 0 \\ (p_x - x_x)^2 + (p_y - x_y)^2 - (p_{zi} - x_z)^2 \tan^2 \phi &= 0 \end{aligned} \quad (17)$$

Here we see that the thirteen (or fifteen) horizontal cutting plane equations  $p_z - p_{zi} = 0$ ,  $i = 1, \dots, 13(15)$  have been incorporated so for each value of  $i$  the difference between the first and second of Eq. 17 yields a linear equation that, when combined with either quadratic in Eq. 17, produces the two points of intersection between circles at each level.

## 5.5 Summary and Review

Examine Fig. 30. Here we see, going counterclockwise from upper-left

- Projection, through successive auxiliary (v/p), of a circle presented in a general conjugate (v/p) pair, to yield first an (e/l) (v/p) of its plane then a (TS) (v/p). Note how (TL) (v/p) of diameters are used together with their conjugates to accomplish all this,
- Piercing point  $G$  between line  $DE$  and plane  $ABC$  segments using a vertical plane -i- on line  $DE$  that cuts  $AB$  at  $P$  and  $BC$  on  $Q$  such that  $G \in PQ \in ABC$  and  $G \in DE$ ,
- A plane (+) to (v/p) -F- that obliquely sections a vertical cylinder of revolution to produce an elliptical trace on major and minor principal axial diameters  $AB$  and  $CD$  and
- How to obtain the four points of intersection, on the quartic curve of intersection between a pair of cylinders of revolution, that occur on a particular horizontal cutting plane. Note that these points appear on coplanar generator pairs on each cylinder.

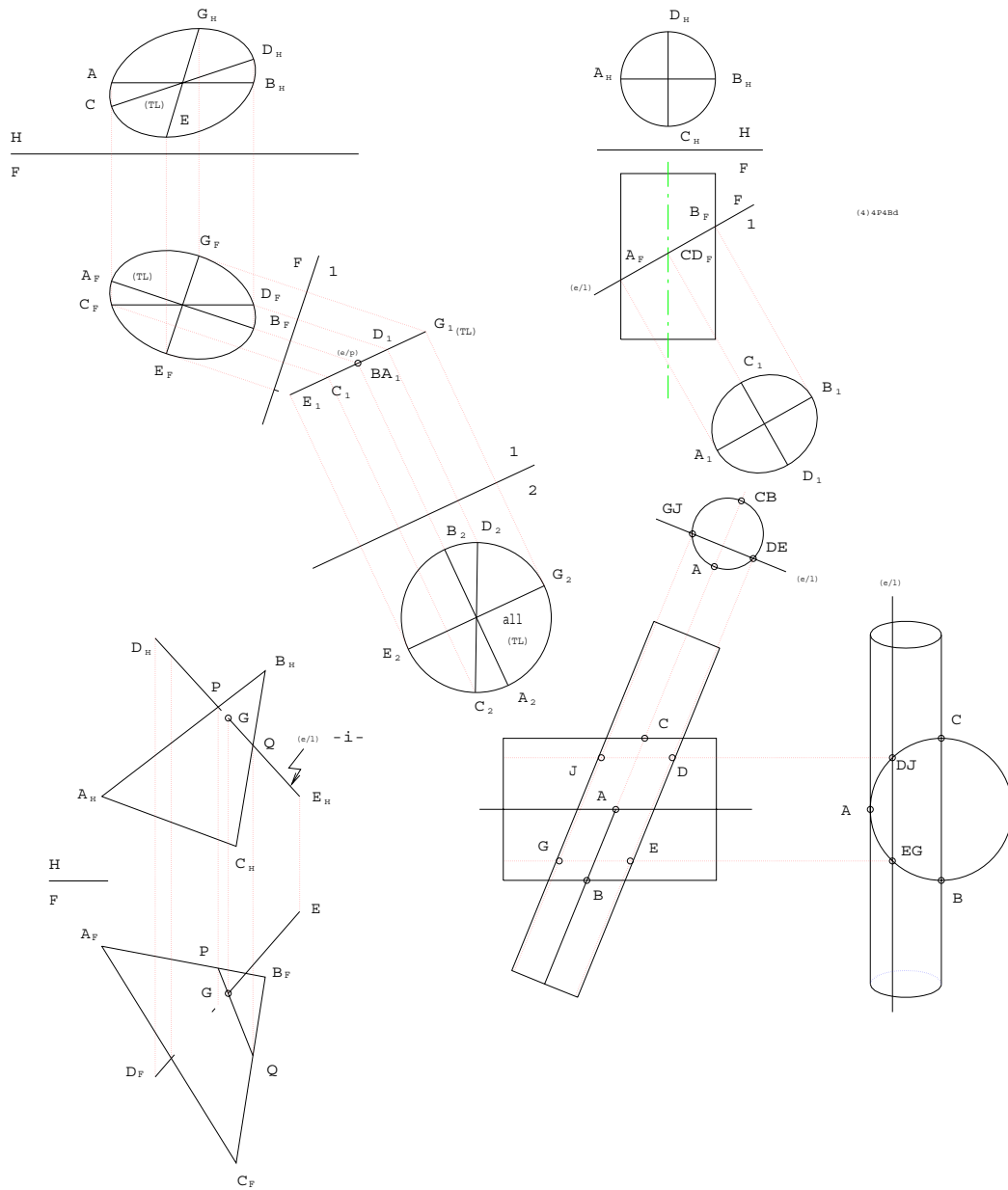


Figure 30: Four Intersections

## 5.6 An Oblique Prop

Fig. 31 shows how to design an oblique prop of rectangular cross section which is constrained by a corner (point A) at the top as well as two cutting planes; a frontal one and a horizontal one at maximum height.

Find the length of the 2x3  
 as well as the swing and tilt  
 angles, all visible in 3rd  
 and 4th auxiliary (v/p)s.

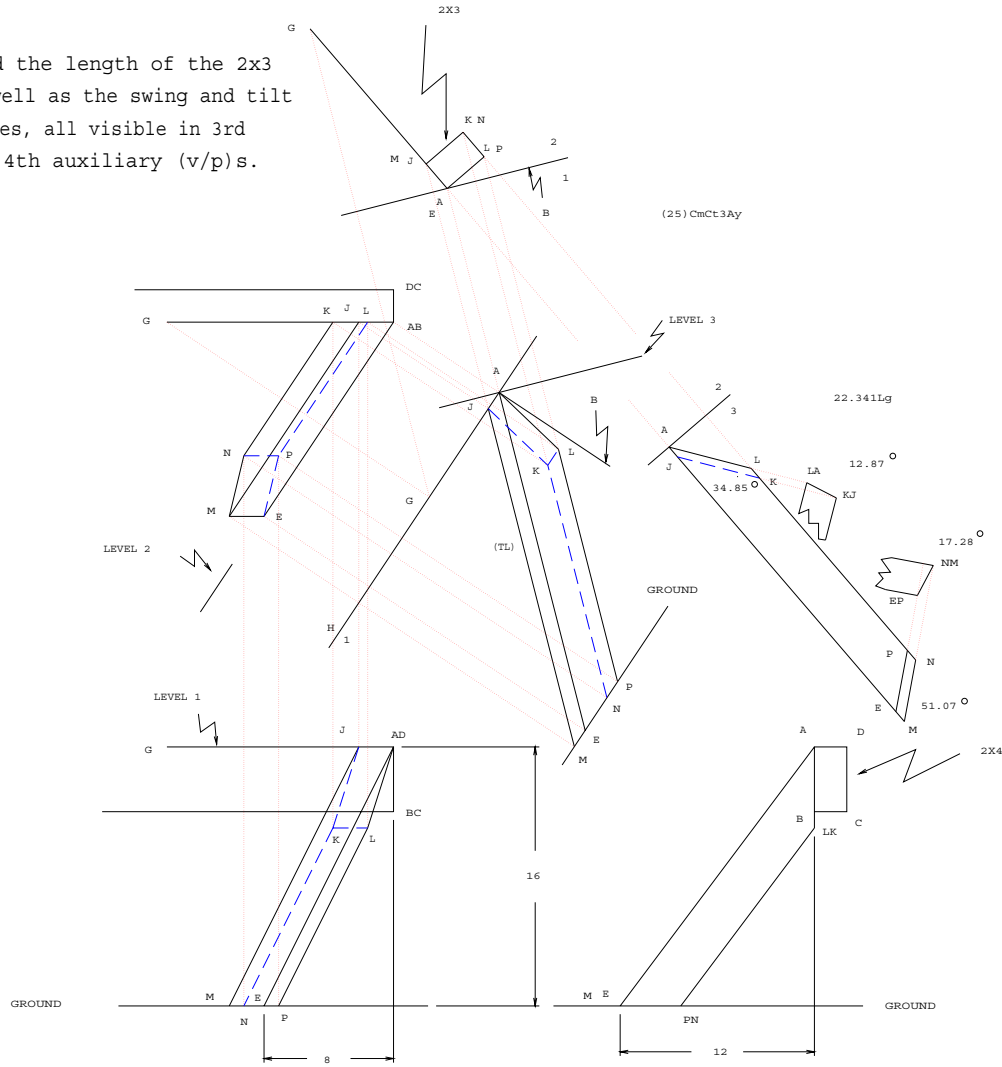


Figure 31: Compound Saw Cuts

The horizontal one defines a LoX on this another edge of the prop is constrained. At the bottom the prop is cut by a floor plane and the point  $E$  is located. The problem is to find all four points of the cut section above  $AJKL$  and the four down below on  $EMNP$ . When this has been done we get a (TS) of the 3-width side of the  $2 \times 3$  to measure the two “swing” angle of saw cut. This is in a  $3^{rd}$  auxiliary (v/p) where (TL) of the  $2 \times 3$  may be measured. Then we get a (TS) of the 2-width side of the  $2 \times 3$  to measure the two “tilt” angle of saw cut. These are in two  $4^{th}$  auxiliary (v/p)s. See how complicated the specification of a rectangular prism, frustrated by two oblique planes can get even though this is just a matter of defining two pairs of traces and dihedral angles?

## 5.7 Development

All surfaces composed of combinations of planar facets and cones, *i.e.*, surfaces ruled by real line generators that all impinge on a common point are “developable”, *i.e.*, can be laid out on a single plane and creased and formed, without stretching, into final desired shape. In general, parts of developables may be defined as swept by a line moving on a fixed point so as to intersect an arbitrary fixed spatial curve. Obviously such definition includes planes and cylinders. The example dealt with and shown in Fig. 32 is composed of four triangular (plane) elements  $AQB$ ,  $BRC$ ,  $CSD$  and  $DPA$  that share line segments as bounding generators of four intermediate ellipsoconical elements  $APQ$ ,  $BQR$ ,  $CRS$  and  $DSP$ .

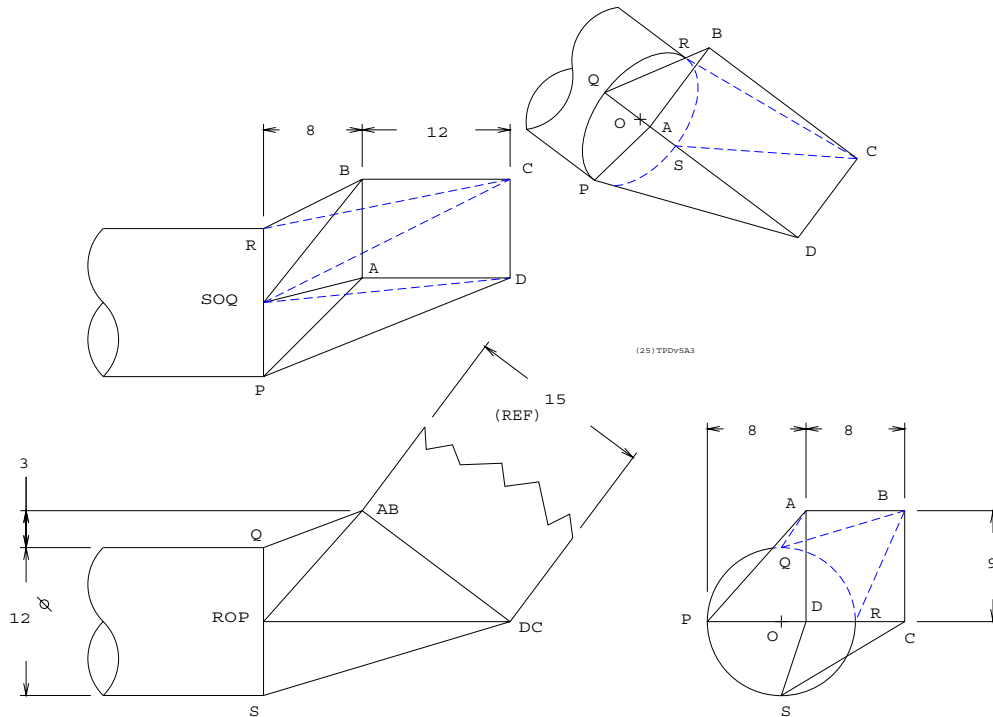


Figure 32: Transition Piece

The purpose of the final shape is to make a connecting span between the circular opening of a duct to another duct’s rectangular opening. This connection is called a transition piece. Planes of the rectangular and circular holes are oblique. The only concession to symmetry, *i.e.*, short of a completely general configuration, is that a pair of rectangular edges are parallel to the plane of the circle. Each quarter circular arc,  $PQ$ ,  $QR$ ,  $RS$  and  $SP$  is divided into arcs of  $\pi/12$  and the lengths of  $7 \times 4$  generators is computed, using the dimensions provided in Fig. 32, by means of the program listed in the table below together with a list of generator lengths taken in a clockwise direction when facing the circular opening.

|     |  |       |          |
|-----|--|-------|----------|
| 100 | PI=3.141592654#:FTD15*PI/180:LA=PI/2:R=6 | APQ 0 | 14.45683 |
| 110 | XA=8:YA=2:ZA=9:XB=8:YB=10:ZB=9           | APQ 1 | 13.42497 |
|     | XC=20:YC=10:ZC=0:XD=20:YD=2:ZD=0         | APQ 2 | 12.32009 |
| 120 | FOR I=0 TO 6                             | APQ 3 | 11.20728 |
| 130 | Y=-R*COS(FTD*I):Z=R*SIN(FTD*I)           | APQ 4 | 10.17198 |
| 140 | LPRINT "APQ";I;" ";SQR(XA*XA+(Y-YA)^2    | APQ 5 | 9.321569 |
|     | +(Z-ZA)^2)                               | APQ 6 | 8.774964 |
| 150 | NEXT I                                   |       |          |
| 160 | LPRINT:REM Transition piece design       | BQR 0 | 13.15295 |
|     | MECH 289, 05-12-13                       | BQR 1 | 12.06738 |
| 170 | FOR I=6 TO 12                            | BQR 2 | 11.29023 |
| 180 | Y=-R*COS(FTD*I):Z=R*SIN(FTD*I)           | BQR 3 | 10.94439 |
| 190 | LPRINT "BQR";I-6;" ";SQR(XB*XB+(Y-YB)^2  | BQR 4 | 11.09401 |
|     | +(Z-ZB)^2)                               | BQR 5 | 11.71053 |
| 200 | NEXT I                                   | BQR 6 | 12.68858 |
| 210 | LPRINT:REM (25)TPDV3B1.BAS               |       |          |
| 220 | FOR I=12-18                              | CRS 0 | 20.39608 |
| 230 | Y=-R*COS(FTD*I):Z=R*SIN(FTD*I)           | CRS 1 | 20.49607 |
| 240 | LPRINT "CRS";I-12;" ";SQR(XC*XC+(Y-YC)^2 | CRS 2 | 20.78646 |
|     | +(Z-ZC)^2)                               | CRS 3 | 21.24023 |
| 250 | NEXT I                                   | CRS 4 | 21.81743 |
| 260 | LPRINT:REM Refer to Fig. 32 (25)TPDV5A3  | CRS 5 | 22.47091 |
| 270 | FOR I=18 TO 24                           | CRS 6 | 23.15168 |
| 280 | Y=-R*COS(FTD*I):Z=R*SIN(FTD*I)           |       |          |
| 290 | LPRINT "DSP";I-18;" ";SQR(XD*XD+(Y-YD)^2 | DSP 0 | 20.97618 |
|     | +(Z-ZD)^2)                               | DSP 1 | 21.12372 |
| 300 | NEXT I                                   | DSP 2 | 21.26029 |
| 310 | STOP:END                                 | DSP 3 | 21.37687 |
|     |  | DSP 4 | 21.46590 |
|     |  | DSP 5 | 21.52167 |
|     |  | DSP 6 | 21.54066 |

Then, with the chord length subtending  $\pi/12$ , the sections of the cone surfaces, each approximated by six narrow triangles, alternate with the planotriangular patches and laid out as shown in Fig. 33.

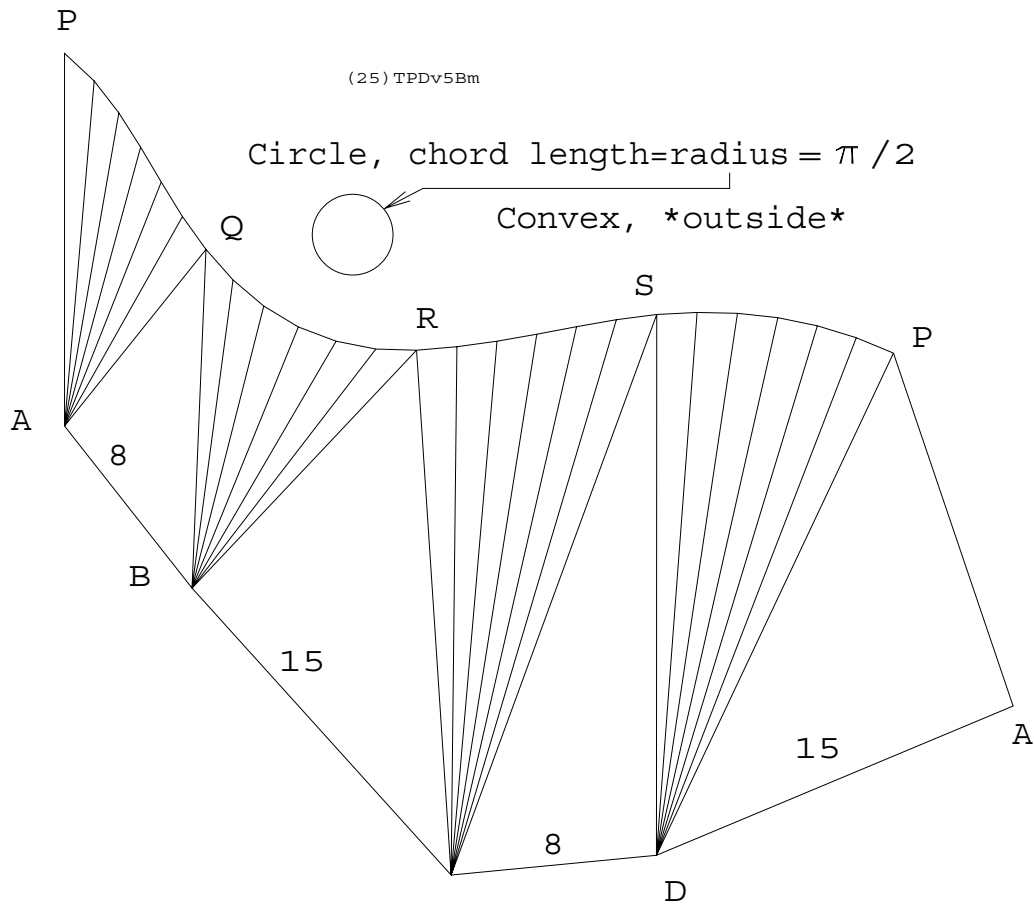


Figure 33: The Development Laid Out Flat

To get things right one must decide at the beginning whether the layout sequence is to be internal or external to the transition piece and take care that no inadvertent “switching of sides” along the way.



## 6 Parametric Curves and Surfaces

“Smooth” curves and surfaces have been part of the designer-engineer’s *répertoire* for centuries. These forms are used wherever their æsthetic or streamlining qualities may be desired. Earliest examples are found in architecture, clothing, footwear, furniture, tools and weapons. Hulls and lifting and control surfaces to efficiently deflect fluid are modern examples and remain the subject of intensive research for the foreseeable future. Very often accurate computational fluid dynamic (CFD) models require expensive and lengthy calculation of flow paths hence these data are computed only at widely spaced, discrete points on a boundary surface. This sometimes applies to other surfaces too, *e.g.*, spatial cam and gear tooth profiles. Nevertheless such sculpted surfaces, not to mention elements of biosystems, are continuous and they or their casting or forging molds must be generated by a cutting tool moving so as to suitably interpolate between established points. This is where notions like natural, Bézier, B-spline and NURBS (nonuniform rational B-spline) curves and surface patches (Ferguson and Coons) come into play. They are quite easy and convenient to compute and give the designer considerable intuitive, sometimes local, control over shape while remaining acceptably faithful to exact shape. The natural or elastic spline will be introduced briefly before delving a bit more deeply into parametric and equivalent Bézier cubic curves and their biparametric surface patch counterparts. This elementary introduction will neither treat B-splines, a way to blend a series of curve “pieces”, nor NURBS that overcome some limitations of B-splines through the application of projective geometry. For example, NURBS include circular, elliptical and hyperbolic arcs. Note that Bézier cubics degenerate to produce perfect parabolic and straight line segments but not other conics. B-spline circles are “lumpy”.

### 6.1 Natural Spline

A natural spline is produced by the elastic bending of a straight wire or thin strip or lath to lie constrained between a series of narrow gaps provided by frictionless peg pairs. The spline may pass as many gap points as one may desire. The set of simultaneous equations, one for each interval between successive gaps, is solvable by imposing an appropriate moment (tangent condition) on the spline at the first and last gap and assuming that only a concentrated force, but no moment, acts at each intermediate gap. All gap point position vectors are specified as desired. For a planar spline the bending equation

$$\frac{d^2y}{dx^2} = \frac{M(x)}{EI} \quad (18)$$

applies to the interval between each adjacent gap pair. There is no loss in generality by assuming  $EI = 1$  since one seeks only the curve geometry and not the magnitude of forces and moments. The Cartesian relation implied by Eq. 18 is valid based on the assumption that, by taking the straight line between adjacent gaps as the local  $x$ -axis, the deflection in direction  $y$ , normal to this, is small compared to gap spacing. Ship builders have been using actual, full scale splines, to frame hulls that are smooth and fair, since time immemorial. Although natural wooden or metal splines can be tweaked at the gaps to accommodate a local, necessary bulge or dent in the hull shape this is not well suited to equation sets composed of Eq. 18.

## 6.2 Drawing a Patch

A patch is a triangular or quad mesh defined on a boundary tri- or quadrilateral of pairwise intersecting space curves. CAD systems embody features to render mesh cells opaque and to shade them. Cell spacing or “fineness” can be varied to suit the size of the image displayed. Fig. 34 shows opaque cells to produce the illusion of depth and multiple curvature on a quadpatch bounded by four cubic edge curves.

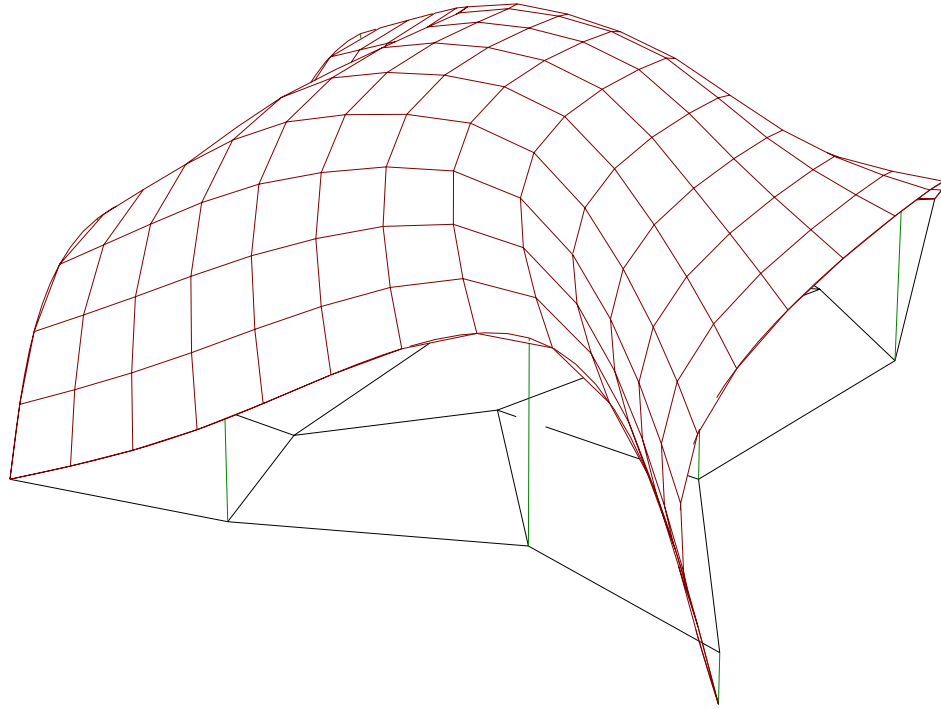


Figure 34: Rendered Quadpatch

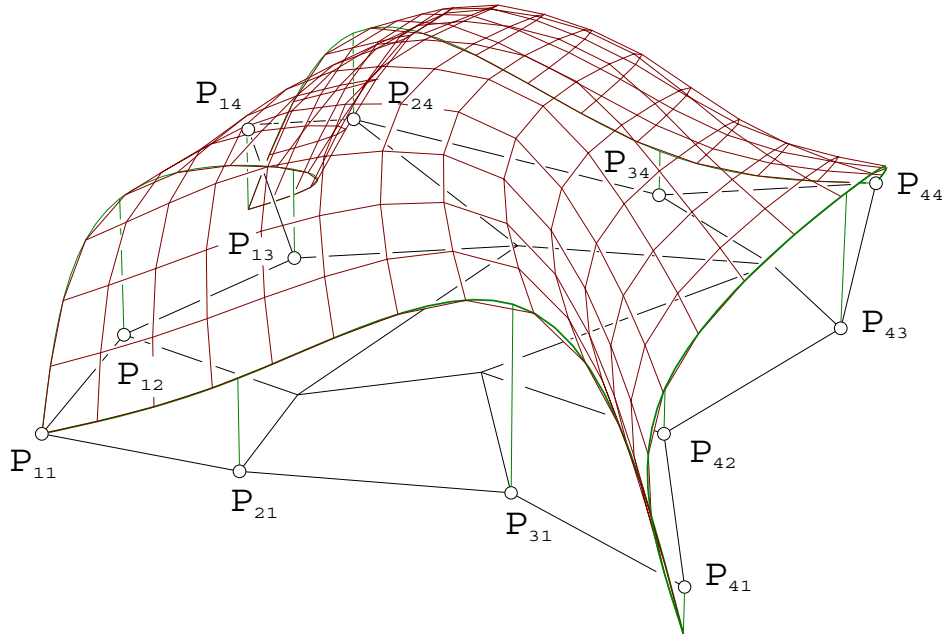


Figure 35: Wire Frame Blended Quadpatch

The underlying structure supporting the  $13 \times 13$  biparametric surface grid is shown more clearly in Fig. 35. The grid is composed of orthogonal cubic characteristics that smoothly interpolate between each pair of nonintersecting boundary curves. Four points on each boundary curve were established by extending verticals from points on a  $3 \times 3$  grid of planar quadrilaterals. Verticals shown extend upward from points  $P_{21}$ ,  $P_{24}$ ,  $P_{31}$ ,  $P_{34}$  and downward from corners  $P_{14}$ ,  $P_{41}$  while  $P_{11}$  and  $P_{44}$  each terminate a pair of boundary curves. From left to right, going clockwise around the planar grid one sees the following points on these curves.

$$\begin{array}{cccc}
 P_{11}(0, 0, 0) & P_{21} \uparrow (4, 0, 2) & P_{31} \uparrow (9, 1, 4) & P_{41} \downarrow (13, -1, -1) \\
 P_{41} \downarrow (13, -1, -1) & P_{42} \uparrow (11, 4, 1) & P_{43} \uparrow (13, 9, 3) & P_{44}(12, 15, 0) \\
 P_{44}(12, 15, 0) & P_{34} \uparrow (8, 13, 1) & P_{24} \uparrow (1, 14, 2) & P_{14} \downarrow (-1, 13, -2) \\
 P_{14} \downarrow (-1, 13, -2) & P_{13} \uparrow (2, 8, 2) & P_{12} \uparrow (0, 4, 3) & P_{11}(0, 0, 0)
 \end{array}$$

After defining the four boundaries, these are “tagged” and the command “patch” is invoked to produce the surface. Note that there are four additional, unlabelled points in the middle of the planar grid. They were not required by the patching procedure but will be seen to have an important rôle in defining a cubic Bézier patch.

### 6.3 Parametric Curves

First, the need for parametric representation will be demonstrated by examining the result of fitting an explicit parabola,  $y = f(x)$ , to a pattern of three given points,  $(0, 0)$ ,  $(1, 1)$ ,  $(2, 1)$ ,

then doing it again after the pattern has been rotated clockwise by  $\frac{\pi}{4}$  and comparing it to an equivalent parameterized conic. Second, parameterized spatial cubic curves will be introduced together with their relationship to Bézier cubics. Finally, de Casteljau’s construction algorithm of Bézier curves and patches will be treated to complete this discussion of “free form” modelling.

### 6.3.1 Parametric Representation

Parameterized representation of straight line segments has already been encountered. The notion is similar when treating parabolic and cubic arcs. The parameter may be imagined as a Cartesian coordinate orthogonal to the Euclidean space in which drawings are made. In the case of curves, parameterization is more than a convenience. Explicit or implicit equations produce curves that may be defined as passing through given points. However the curve shape is changed if the supporting pattern of points is rotated. Shape of a drawn object must not be altered at the whim of coordinate axis choice. Consider the three parabolæ shown in Fig. 36.

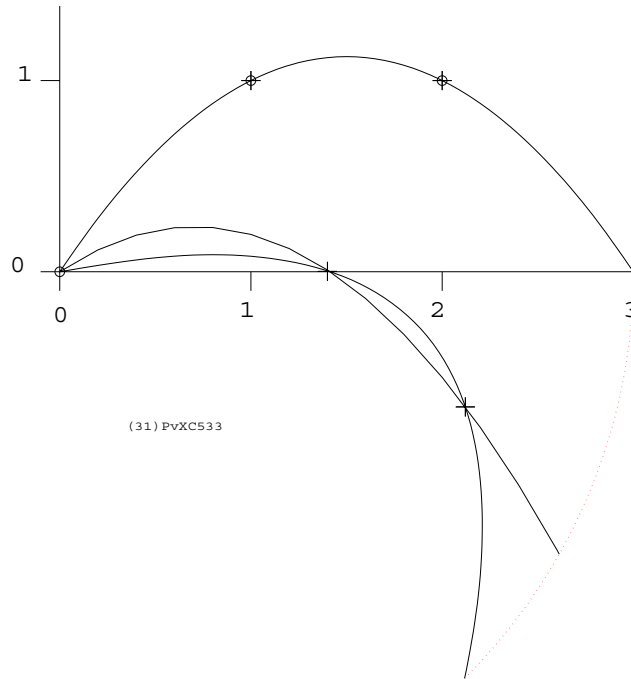


Figure 36: Explicit and Parametric Conics under Rotation

The first was drawn on the three points given above. Then these were rotated clockwise about the origin. Original  $y$  and rotated  $y_r$  point pattern explicit equations are written below.

$$y = -\frac{1}{2}x^2 + \frac{3}{2}x, \quad y_r = -\frac{1}{3}\sqrt{2}x^2 + \frac{2}{3}x$$

When the point pattern rotated the curve did not. The vertex moved lower, to the left. The original explicit and unrotated parametric curves are identical. The rotated parametric curve behaves as if it and the three points on it were simply rotated about the origin. In the case of the explicit curve, the three points remain on it but have slid along the curve as if the “glue” became unstuck. How was the parametric curve formulated?

- The parameter  $u$  assumes three values that correspond to the three given points. For convenience

$$(0, 0) \equiv u = 0, \quad (1, 1) \equiv u = \frac{1}{2}, \quad (2, 1) \equiv u = 1$$

was chosen.

- Second order equations  $x = x(u)$  and  $y = y(u)$  are defined by

$$[\mathbf{P}] = [\mathbf{A}][\mathbf{U}] \quad (19)$$

where  $[\mathbf{P}]$  is a  $2 \times 3$  matrix of the three given planar point position vectors,  $[\mathbf{A}]$  is a  $2 \times 3$  coefficient matrix whose elements are to be determined and  $[\mathbf{U}]$  is a  $3 \times 3$  matrix whose columns are formed as  $[u^0 \ u^1 \ u^2]^T$  using the three values of  $u$  chosen to correspond to the given point position vectors. Eq. 19 expands to become Eq. 20.

$$\begin{bmatrix} 0 & 1 & 2 \\ 0 & 1 & 1 \end{bmatrix} = \begin{bmatrix} a_{x0} & a_{xh} & a_{x1} \\ a_{y0} & a_{yh} & a_{y1} \end{bmatrix} \begin{bmatrix} 1 & 1 & 1 \\ 0 & \frac{1}{2} & 1 \\ 0 & \frac{1}{4} & 1 \end{bmatrix} \quad (20)$$

- Postmultiplying both sides of Eq. 20 by  $[\mathbf{U}]^{-1}$  yields  $[\mathbf{A}]$ . Then any value of a vector  $\mathbf{u}$  will produce a corresponding point  $P$  on the curve where vector  $\mathbf{p}$  is the position vector.

$$\mathbf{p} = [\mathbf{A}]\mathbf{u}, \quad \begin{bmatrix} p_x \\ p_y \end{bmatrix} = \begin{bmatrix} 0 & 2 & 0 \\ 0 & 3 & -2 \end{bmatrix} \begin{bmatrix} u^0 \\ u^1 \\ u^2 \end{bmatrix} \quad (21)$$

To produce the curve, Eq. 21 is solved at sufficiently small increments of  $u$  in the desired range.

- As an exercise, find  $[\mathbf{A}]$  for

$$[\mathbf{P}] = \begin{bmatrix} 0 & \sqrt{2} & \frac{3\sqrt{2}}{2} \\ 0 & 0 & -\frac{\sqrt{2}}{2} \end{bmatrix}$$

the clockwise rotated pattern of points.

### 6.3.2 Cubic and Higher Geometric Forms

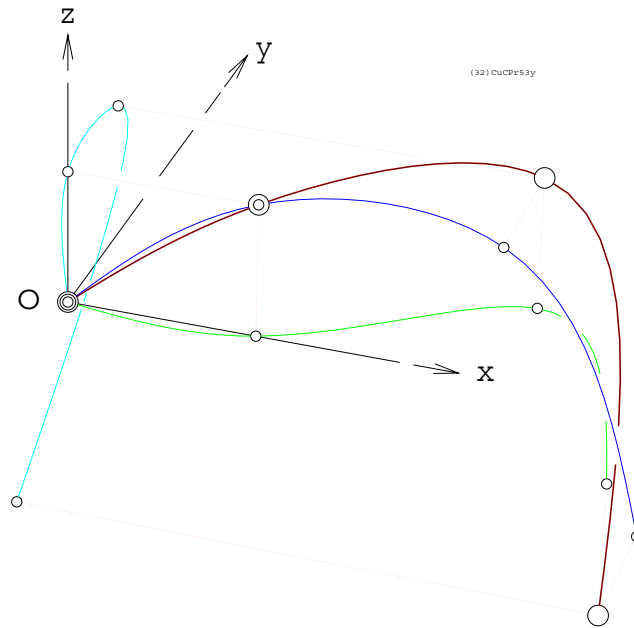


Figure 37: Parametric Cubic Curve and Principal Projections

As may be grasped by examining Fig. 29 a spatial curve is described by two, not one, implicit equations. Equations of second order represent such quadric surfaces. The curve in that case is of fourth degree since it may intersect a plane in four places. Note that the surfaces are of second order because a straight line may intersect them but twice. All curves of second degree are conics, *i.e.*, planar. By resorting to parametric *cubics*, curves of third degree, twist or bending out of a plane is introduced because the third derivative of a cubic univariate equation survives as a constant. Cubics are curves of constant twist. Before getting into details, look at Fig. 37. It was drawn on a sequence of four supporting points.

$$(0, 0, 0), (4, 0, 3), (9, 3, 3), (12, -3, -3)$$

In the CAD environment these points were “set” and the icon representing “curve” was clicked upon; presto! What happened? We don’t know for sure but let’s hypothesize by building on the surface intersection paradigm. Imagine the three planar cubic curves on the three principal projections of these four points.

$$\begin{array}{cccc} (0, 0, 0) & (0, 0, 3) & (0, 3, 3) & (0, -3, -3) \\ (0, 0, 0) & (4, 0, 3) & (9, 0, 3) & (12, 0, -3) \\ (0, 0, 0) & (4, 0, 0) & (9, 3, 0) & (12, -3, 0) \end{array}$$

Now any of these curves could be drawn parametrically as planar cubics according to the examples of Eqs. 19, 20 and 21 except that  $[\mathbf{P}]$ ,  $[\mathbf{A}]$  and  $[\mathbf{U}]$  would assume dimensions  $2 \times 4$ ,  $2 \times 4$  and  $4 \times 4$ , respectively. One might represent each set of four point projections as

parameterized on the sequence  $u = 0, \frac{1}{3}, \frac{2}{3}, 1$ . Then imagine the intersection of the orthogonal cylinders produced by extruding the cubics on  $y = 0$  and  $z = 0$ . A third cylinder on  $x = 0$  would intersect on the same spatial curve depicted. The process with two cylinders is not necessary. Results can be combined into Eq. 22. Notice the rôle of the so called geometric to algebraic form transformation matrix  $[\mathbf{U}]_{4P}^{-1}$ .

$$\begin{bmatrix} p_x(u) \\ p_y(u) \\ p_z(u) \end{bmatrix} = \begin{bmatrix} p_{0x} & p_{13x} & p_{23x} & p_{1x} \\ p_{0y} & p_{13y} & p_{23y} & p_{1y} \\ p_{0z} & p_{13z} & p_{23z} & p_{1z} \end{bmatrix} \begin{bmatrix} 1 & 1 & 1 & 1 \\ 0 & \frac{1}{3} & \frac{2}{3} & 1 \\ 0 & \frac{1}{9} & \frac{4}{9} & 1 \\ 0 & \frac{1}{27} & \frac{8}{27} & 1 \end{bmatrix}^{-1} \begin{bmatrix} u^0 \\ u^1 \\ u^2 \\ u^3 \end{bmatrix} \quad (22)$$

### 6.3.3 Standard Geometric Form

To see how the two families of characteristics shown in Fig. 35 might be generated to produce the rendered image in Fig. 34, as described in section 6.2, one must consider how the necessary information provided by four internal, unlabelled points  $P_{22}, P_{23}, P_{32}, P_{33}$  of the  $3 \times 3$  grid can be obtained. But first an alternate way to represent spatial curves like that in Fig. 37 must be introduced. An identical curve can be produced by specifying *any* four constraints consisting of point position vectors and their first and second derivatives with respect to the parameter  $u$ . *E.g.*, the intermediate two points may be replaced by tangent vectors at  $u = 0$  and  $u = 1$  (first derivatives), at the initial and terminal points on the curve. This is natural when concatenating two curve segments with matching slope. This definition of a parametric cubic is called “standard geometric form” (SGF). As a preliminary exercise we show how to produce the two tangent vectors  $\mathbf{p}^u(0)$  and  $\mathbf{p}^u(1)$ . The curve is defined by its algebraic coefficient matrix  $[\mathbf{A}]$  and the first derivative of the cubic parameter vector  $[u^0 \ u^1 \ u^2 \ u^3]$  is  $[0 \ u^0 \ 2u^1 \ 3u^2]$  so

$$\begin{aligned} [\mathbf{A}] &= [\mathbf{P}]_{4P} [\mathbf{U}]_{4P}^{-1} = [\mathbf{P}]_{SGF} [\mathbf{U}]_{SGF}^{-1} \\ [\mathbf{P}]_{SGF} &= [\mathbf{P}]_{4P} [\mathbf{U}]_{4P}^{-1} [\mathbf{U}]_{SGF} \end{aligned} \quad (23)$$

or for the curve in Fig. 37

$$\begin{aligned} \begin{bmatrix} p_{0x} & p_{0x}^u & p_{1x} & p_{1x}^u \\ p_{0y} & p_{0y}^u & p_{1y} & p_{1y}^u \\ p_{0z} & p_{0z}^u & p_{1z} & p_{1z}^u \end{bmatrix} &= \begin{bmatrix} 0 & \frac{15}{2} & 12 & 3 \\ 0 & -\frac{33}{2} & -3 & -\frac{87}{2} \\ 0 & \frac{21}{2} & -3 & -30 \end{bmatrix} \\ &= \begin{bmatrix} 0 & 4 & 9 & 12 \\ 0 & 0 & 3 & -3 \\ 0 & 3 & 3 & -3 \end{bmatrix} \begin{bmatrix} 1 & -\frac{11}{2} & 9 & -\frac{9}{2} \\ 0 & 9 & -\frac{45}{2} & \frac{27}{2} \\ 0 & -\frac{9}{2} & 18 & -\frac{27}{2} \\ 0 & 1 & -\frac{9}{2} & \frac{9}{2} \end{bmatrix} \begin{bmatrix} 1 & 0 & 1 & 0 \\ 0 & 1 & 1 & 1 \\ 0 & 0 & 1 & 2 \\ 0 & 0 & 1 & 3 \end{bmatrix} \end{aligned} \quad (24)$$

Notice that the first and third column vectors in the top line of Eq. 24 have been preserved to contain the initial and terminal point positions of the curve. The second and last columns

are the tangent vectors at these points. Vectors of exactly  $\frac{1}{3}$  of the magnitude of these tangent vectors locate the intermediate cubic Bézier control points, subtended forward and backward from the initial and terminal points of the curve segment. Later we will see how the four missing internal points, mentioned in connection with quadpatch shown in Fig. 34, are obtained using the notions exposed above. Naturally the user can blissfully ignore what happens when clicking upon the “patch” icon.

### 6.3.4 Bézier Curve and Quadpatch

Now look at the 3 cell mesh of twisted quadrilateral cells shown in Fig. 38(a). this is similar to but *not* the same one shown in Figs. 35 and 34.

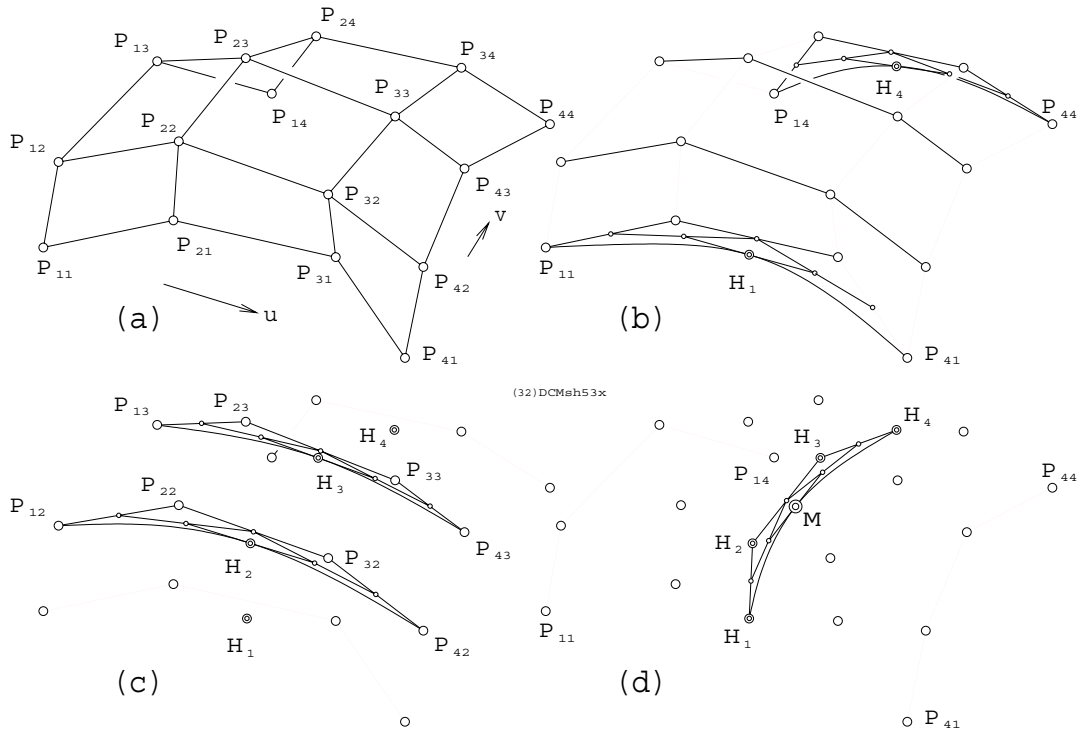


Figure 38: De Casteljau’s Constructions of Cubic Bézier Curves and Surfaces

The four corner points  $P_{11}, P_{14}, P_{41}, P_{44}$  are boundary curve segment terminal points and not projected from points on any planar grid. Furthermore the intermediate point pairs along the boundaries are not on the curve. These are the Bézier control points that may be obtained from a four point representation of the boundary curves that are not shown.

$$P_{12}, P_{13}, P_{21}, P_{31}, P_{24}, P_{34}, P_{42}, P_{43}$$

are generated by applying Eq. 23 to each boundary curve, each defined, possibly, with four given points. After these have been obtained the boundary curves are approximated by



incrementing  $u = 0 \rightarrow 1$  using de Casteljau’s algorithm, illustrated by geometric construction in Fig. 38(b). This construction provides insight into its algorithmic derivative leading to highly efficient computation because it is naturally suited to acceleration available with parallel and pipelined processor architecture. Although details of that are peripheral to a graphics course, the elegantly simple construction is quite appropriate. See how  $H_1$  and  $H_4$  were constructed for the specific value of  $u = 0.5$ . Assuming  $\mathbf{p}_{ij}$  is the position of a node on the mesh one may immediately write the expression for the position vector of  $\mathbf{h}_i$ .

$$\begin{aligned}
 \mathbf{q}_1 &= \mathbf{p}_{11} + 0.5(\mathbf{p}_{21} - \mathbf{p}_{11}) \\
 \mathbf{q}_1 &= \mathbf{p}_{21} + 0.5(\mathbf{p}_{31} - \mathbf{p}_{21}) \\
 \mathbf{q}_1 &= \mathbf{p}_{31} + 0.5(\mathbf{p}_{41} - \mathbf{p}_{31}) \\
 \mathbf{r}_1 &= \mathbf{q}_1 + 0.5(\mathbf{q}_2 - \mathbf{q}_1) \\
 \mathbf{r}_2 &= \mathbf{q}_2 + 0.5(\mathbf{q}_3 - \mathbf{q}_2) \\
 \mathbf{h}_1 &= \mathbf{r}_1 + 0.5(\mathbf{r}_2 - \mathbf{r}_1)
 \end{aligned} \tag{25}$$

Thus the four boundary curves can be drawn. What about the the two families of characteristics that blend between the two opposite edge pairs? The first step, to get the four internal Bézier control points, is illustrated in Fig. 39. Notice how the terminal tangent vectors at corners points have been reversed, as required, to point “inward”.

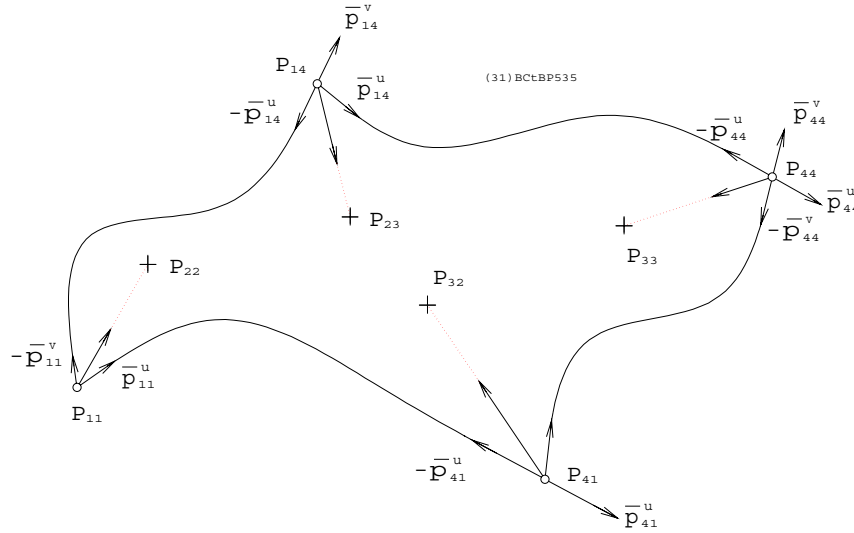


Figure 39: Tangent Vector Sums Define Internal Bézier Control Points

$$\begin{aligned}
 \mathbf{p}_{22} &= \mathbf{p}_{11} + (\mathbf{p}_{11}^u + \mathbf{p}_{11}^v)/3, & \mathbf{p}_{23} &= \mathbf{p}_{14} + (\mathbf{p}_{14}^u - \mathbf{p}_{11}^v)/3 \\
 \mathbf{p}_{32} &= \mathbf{p}_{41} - (\mathbf{p}_{41}^u - \mathbf{p}_{41}^v)/3, & \mathbf{p}_{33} &= \mathbf{p}_{44} - (\mathbf{p}_{44}^u + \mathbf{p}_{44}^v)/3
 \end{aligned} \tag{26}$$

Now comes a tricky part. Examine Fig. 38(c). With the internal points produced with Eq. 26 and the two Bézier points of boundary curves, four more Bézier curves are drawn. The two, by incrementing in the “ $u$ ” direction are shown. The de Casteljau algorithm produces as many points along these four curves as may be required. Points  $H_2$  and  $H_3$  are examples, again, when  $u = 0.5$  is set. But these are curves containing Bézier points, not points on actual surface characteristics. However since  $H_1, H_2, H_3, H_4$  are now available, an actual curve on the surface at  $u = 0.5$  can be produced by incrementing  $v$  as shown in Fig. 38(d). A specific point  $M$  at  $u = v = 0.5$  is shown. The whole family is produced by iterating  $u$  “slow”, *i.e.*, the outer computational loop, and  $v$  “fast” in the inner loop. The other family is drawn by iterating  $u$  in the inner loop. After digesting this fairly lengthy but elementary treatment of CAD surface modelling, the student should be well prepared to attack the intricacies of parametrics of higher degree, *viz.*, fifth and seventh, that offer second and third derivative vector control on curve end points so as to properly connect segments that abut with continuous curvature and twist. These are equivalent to six and eight point curves. Even degree curves are avoided because they do not allow an equal number of terminal point constraints to be imposed at each end and any advantage gained on one side would be absent on the other. NURBS have been omitted. They are based on affine transformations that will be the subject of a second geometry course, MECH 576.

# 7 Joining Line Problems

Design of mechanical systems as well as structures, excavations, mines and other earthworks often requires the joining of two given lines in space, *e.g.*, centre lines, with a third line segment whose direction requires the specification of two constraining conditions. This is a ubiquitous and important engineering design situation. Examine Figs. 40 and 41. At left is a top (H) and front (F) descriptive geometric view pair showing a pair of line segments  $AB$  and  $CD$ . Five common ways to specify the connecting direction will be dealt with from constructive as well as algebraic geometric points of view. These are enumerated below.

1. Fig. 40 illustrates the following three connection specifications.

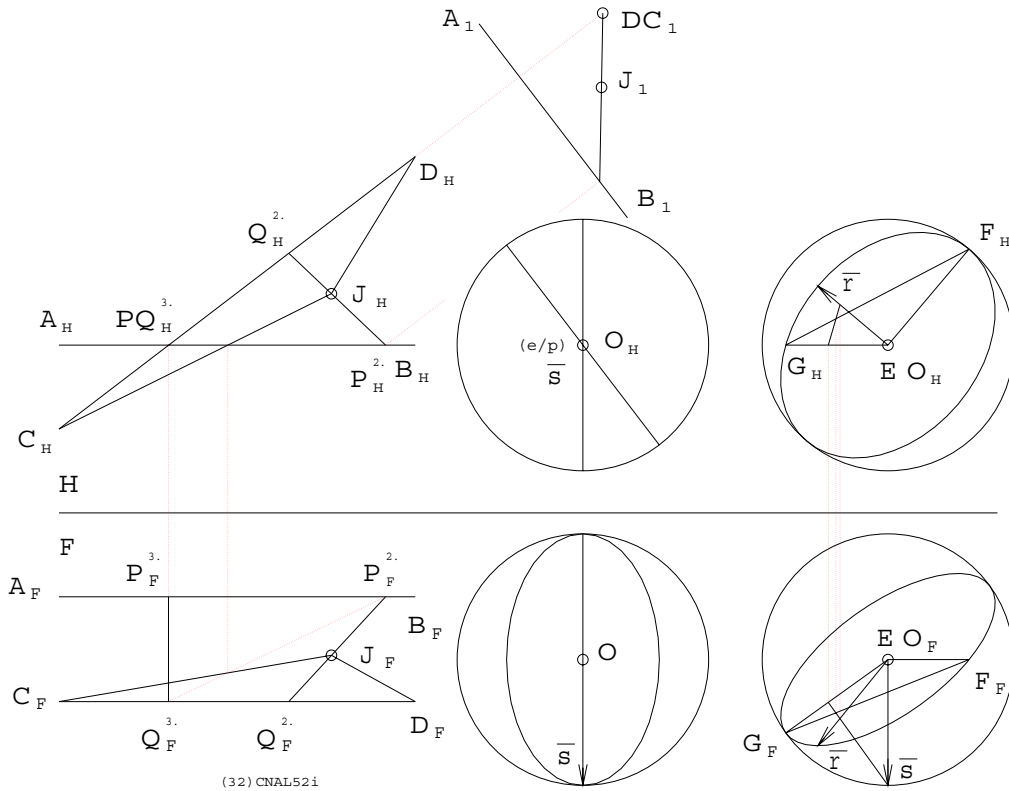


Figure 40: First Three of Five Ways to Connect Two Lines

2. The connection on some given point is on a plane on that point and either given line as well as on the intersection of the other line on that plane.
3. The connection of minimum length is parallel to the perpendicular common to both lines.
4. The direction of shortest connection that is also parallel to a given plane or normal to a given line is the projection of the common perpendicular on that plane.

5. Fig. 41 illustrates the last two connection specifications.

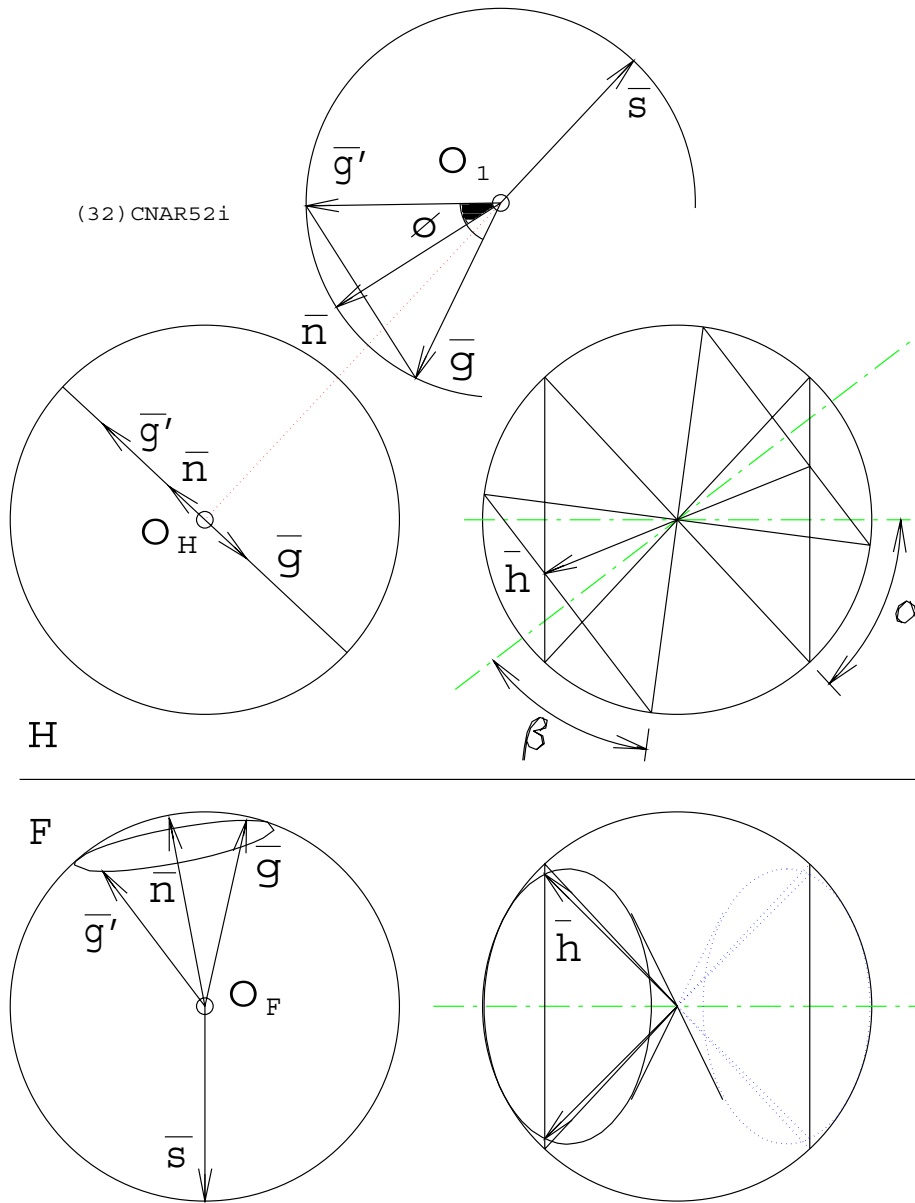


Figure 41: Last Two of Five Ways to Connect Two Lines

6. The direction of shortest connection that makes a specified angle to a given plane or to a given line is the projection of the common perpendicular on the surface of a cone of revolution whose base angle or apex half angle, respectively, is the one specified.
7. The connection that makes a specified angle respective to each given line is in the direction of generators common to two cones of revolution on a common apex, with respective axes parallel to those lines and with apex half angles as specified.

## 7.1 Making the Connection

Once the connecting direction, given by a unit vector  $\mathbf{k}$ , is determined, some point on the connecting line segment  $PQ$ , where  $P$  is on  $AB$  and  $Q$  is on  $CD$ , can be found by defining a plane on, say,  $AB$  and an intersecting line parallel to  $\mathbf{k}$ . The required point is  $Q$  where  $CD$  intersects this plane. This “kernel” procedure is illustrated in Fig. 42

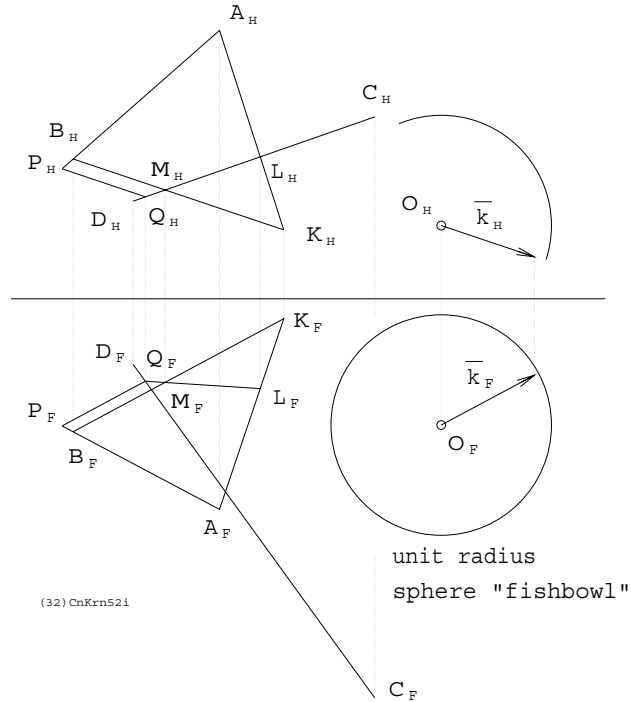


Figure 42: “Kernel” Procedure: To Connect  $AB$  and  $CD$  with  $PQ$  Parallel to  $\mathbf{k}$

The plane segment  $ABK$  contains side  $BK \parallel \mathbf{k}$ . A vertical cutting plane on  $CD$  and intersects  $AK$  on  $L$  and  $BK$  on  $M$ .  $LM$  intersects  $CD$  on  $Q$ , as required. Algebraically, the same procedure is carried out with three simultaneous linear vector equations in unknown scalars  $t$ ,  $u$  and  $k$ . Point position vectors are specified as  $\mathbf{a} = A$ ,  $\mathbf{b} = B$ ,  $\mathbf{c} = C$ ,  $\mathbf{d} = D$ ,  $\mathbf{p} = P$ ,  $\mathbf{q} = Q$ .

$$\mathbf{p} = \mathbf{a} + t(\mathbf{b} - \mathbf{a}), \quad \mathbf{q} = \mathbf{c} + u(\mathbf{d} - \mathbf{c}), \quad \mathbf{k} = k(\mathbf{q} - \mathbf{p}) \quad (27)$$

## 7.2 Connection on a Given Point

This case is subject to geometric reasoning that leads, not to the required direction which would be visible if the views were rotated to show coincidence of the given point  $J$  with the crossing of  $AB$  and  $CD$ , but to a modification to the kernel procedure. If, for example, the plane segment  $CDJ$  is constructed and intersected with  $AB$  that point of intersection

is  $P$ , can be joined to  $J$  and continued to  $Q$  on  $CD$ . Again this involves three simultaneous equations.

$$\mathbf{p} = \mathbf{a} + t(\mathbf{b} - \mathbf{a}), \quad \mathbf{q} = \mathbf{c} + u(\mathbf{d} - \mathbf{c}), \quad \mathbf{j} = j(\mathbf{q} - \mathbf{p}) \quad (28)$$

### 7.3 Parametric Line Equations

Although Eqs. 27 and 28 appear to be virtually identical sets of three there is subtle and important difference in geometric interpretation. In the first instance  $k$  is the fractional distance between  $P$  and  $Q$  that corresponds to unit length. In Eq. 28  $j$  is the distance along  $PQ$  from  $P$  to  $J$  expressed as a fraction of length  $PQ$ . Parametric equations of lines in space are useful in visualizing where a point on a line is with respect to two points on the line. For practice, imagine where  $P$  is if  $t = 0, 1, 0.5, -1, 2$ . Algebraic geometry, or geometric algebra if you prefer, makes use of equations that provide powerful spatial insight into the problems they describe. The parametric line equation is an elementary but highly effective introduction to this art.

### 7.4 Direction for Minimum Length

Examine, now, the first “fishbowl” to the right of the two views of  $AB$  and  $CD$  in Fig. 40. The shortest connection is shown immediately as the vertical line connecting  $AB$  to  $CD$  and visible as the point where  $AB$  crosses over  $CD$  in the top view. However the geometric argument to obtain  $\mathbf{s} = \mathbf{k}$  is that the common perpendicular to the two lines must be in the direction of the line of intersection on *any* two planes respectively normal to the given lines. Both such planes appear in line view in the upper fishbowl. In the front view one sees the meridial traces of the two planes. The one normal to  $AB$  is coincident with the limb of the sphere. The one normal to  $CD$  projects as an ellipse whose major axis is the line of intersection we seek. Algebraically we may write

$$\mathbf{s} = \frac{(\mathbf{b} - \mathbf{a}) \times (\mathbf{d} - \mathbf{c})}{\|(\mathbf{b} - \mathbf{a}) \times (\mathbf{d} - \mathbf{c})\|} \quad (29)$$

### 7.5 Shortest Connection Parallel to a Plane

Sometimes it is desirable to insert a connecting pipe between, say, two skew pipes such that it can be supported on a wall by brackets of equal length or, conversely, with one that juts normally from a column. Both of these possibilities are shown in Fig. 43. Note that points  $P$  and  $Q$  are on two skew lines that are in the direction of unit vector  $\mathbf{r}$  but not shown.

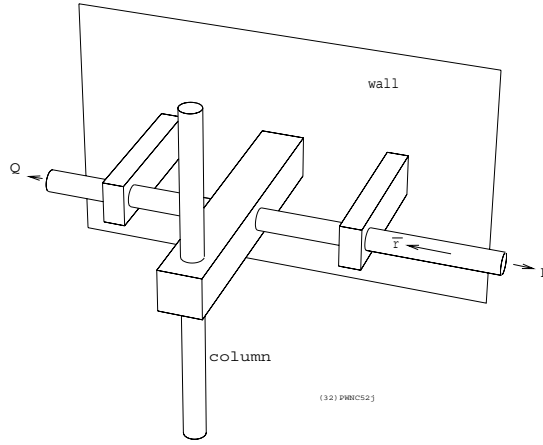


Figure 43: Parallel to Wall or Normal to Column

To visualize the required direction  $\mathbf{r}$  examine the second fishbowl on Fig. 40. Elliptical projections of the circular trace of the wall plane are evident. Inscribed in that is a triangular segment, with unlabelled vertices  $E$ ,  $F$  and  $G$ , onto which  $\mathbf{s}$ , the common normal direction, is projected to produce  $\mathbf{r}$ . Equivalent algebraic reasoning is outlined as follows.

$$\mathbf{n} = (\mathbf{f} - \mathbf{e}) \times (\mathbf{g} - \mathbf{f}), \quad \mathbf{r} = \frac{\mathbf{n} - (\mathbf{n} \cdot \mathbf{s})\mathbf{s}}{\|\mathbf{n} - (\mathbf{n} \cdot \mathbf{s})\mathbf{s}\|} \quad (30)$$

## 7.6 Limiting Connections at a Specified Angle to a Plane

Assume that the economy of a short ramp, between, say, two roadways that intersect at a viaduct, must be limited by some maximum slope or steepness of grade. One desires the shortest connection that makes some specified angle  $\frac{\pi}{2} - \phi$  with respect to some, in this case horizontal, plane. This means that a cone of revolution containing all possible connecting line directions may be imagined. That cone has an axial direction  $\mathbf{n}$  perpendicular to the plane from which the slope is measured. The apex half angle is, of course,  $\phi$ . The cone apex is centred in the third fishbowl and the plane common to the shortest and plane normal unit vectors,  $\mathbf{s}$  and  $\mathbf{n}$ , radiating from the sphere centre intersects the cone in two unit vectors  $\mathbf{g}$  and  $\mathbf{g}'$ . Clearly  $\mathbf{g}$  provides the shortest connecting direction because, among all cone generators, it makes the smallest *acute* angle with  $\mathbf{s}$  and thus affords the greatest component length in the direction of the common normal.  $\mathbf{g}$  and  $\mathbf{g}'$  are obtained with the solution of the following three equations, Eq. 31.

$$\mathbf{n} \cdot \mathbf{g} - \cos \phi = 0, \quad (\mathbf{n} \times \mathbf{s}) \cdot \mathbf{g} = 0, \quad \mathbf{g}^2 - 1 = 0 \quad (31)$$

## 7.7 Connections at Specified Angle to Each Line

The fourth and rightmost fishbowl contains two cones of revolution on a common apex at the sphere centre. The cone axes are respectively parallel to  $AB$  and  $CD$ , the given lines.

These are described by unit vectors  $\mathbf{x}$  and  $\mathbf{y}$ , shown as centrelines. Furthermore the cones have respective apex half angles  $\alpha$  and  $\beta$ . The desired connection must make an angle  $\alpha$  with  $AB$  and  $\beta$  with  $CD$ . Notice how easy it is to identify  $\mathbf{h}$ , one of the two *real* generators common to both cones, hence fulfilling both direction conditions required of the connecting lines. The three necessary constraint equations, Eq. 32, that admit up to four real solutions, not two, are equally easy to formulate.

$$\mathbf{x} \cdot \mathbf{h} - \cos \alpha = 0, \quad \mathbf{y} \cdot \mathbf{h} - \cos \beta = 0, \quad \mathbf{h}^2 - 1 = 0 \quad (32)$$

In order to appreciate the nature of the geometric construction, that is used to find up to four possible directions of connecting line that makes the specified angle with respect to the given skew lines, look at Fig. 44.

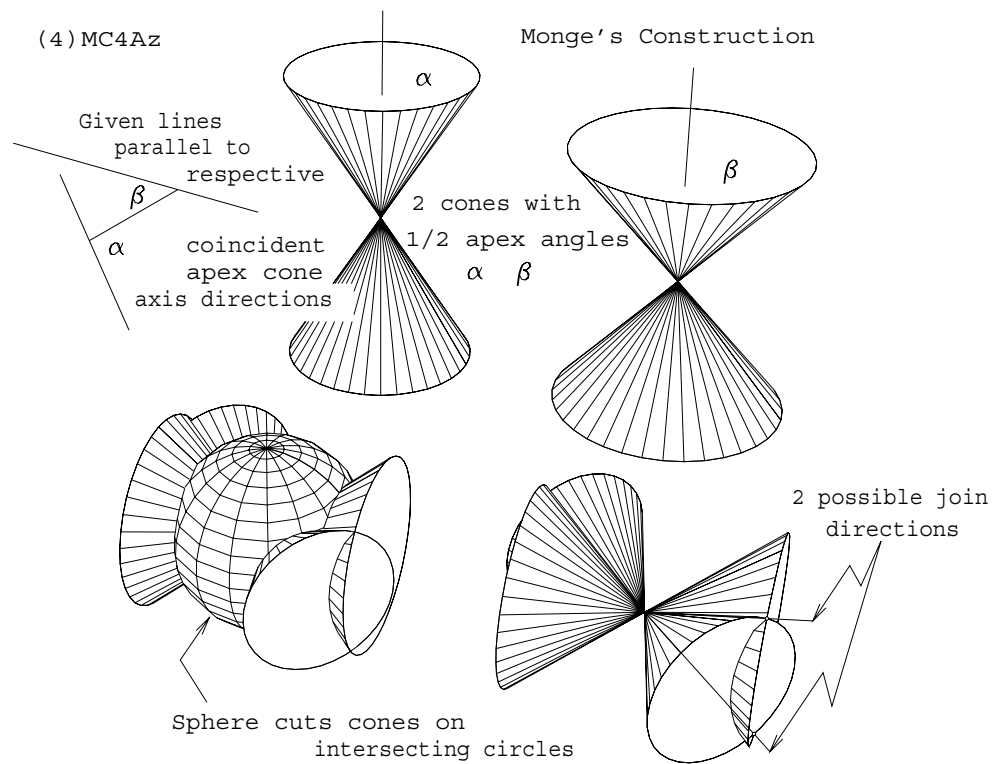


Figure 44: Describing the Cone-Sphere Intersections Engendered in Monge's Construction

Note how the two cones of revolution on a common apex at the sphere centre intersect on a pair of lines (generators) and how the curves of intersection between cone and sphere are circles, *i.e.*, planar curves. Notice also that the given skew lines -to be connected- prescribe the cones' axis directions. Though the circles themselves are not coplanar they intersect on the sphere surface exactly where the two generators, common to both cones, pierce the sphere



surface. Returning to descriptive projection pairs, Fig. 45 shows combinations of given skew line directions and connection angles  $\alpha$  and  $\beta$  that lead, respectively to zero, one, two, three and four possible connections.

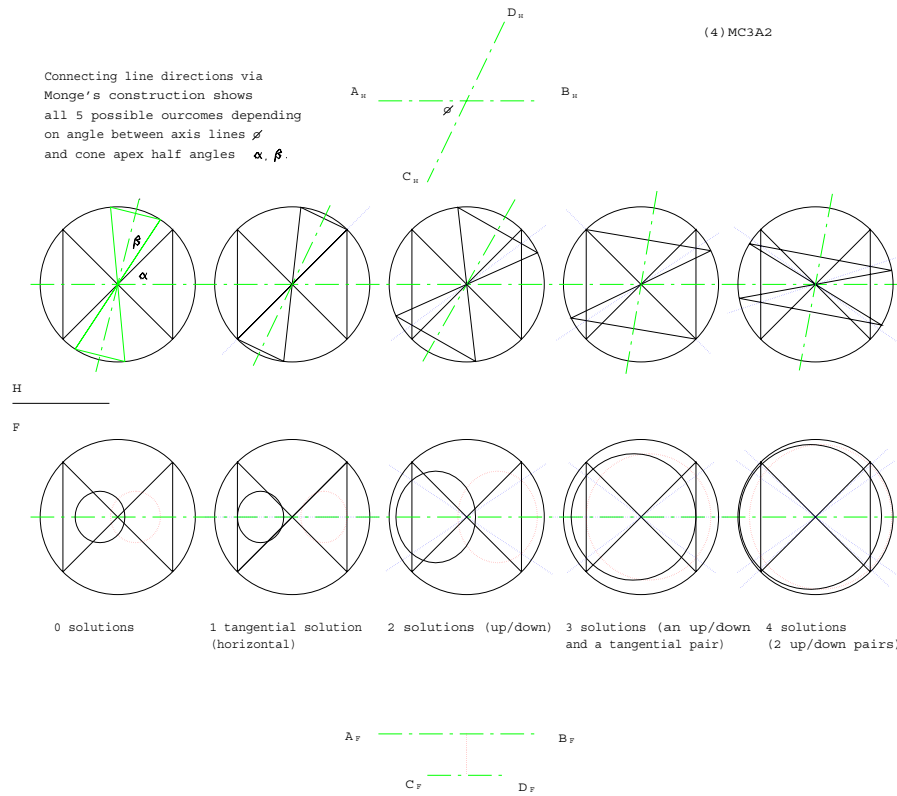


Figure 45: Configurations that Admit 1, 2, 3, and 4 Connections

## 7.8 Problems

### 7.8.1 An Easy One: Bearing Balls

Consider a narrow V-slot cut into a horizontal plate. If the V half angle is  $\alpha$  and the diameter of a typical bearing ball is  $d$  how far from the V apex, along the bisector must a ball roll until it falls through? Illustrate your solution appropriately, *i.e.*, as if you were preparing this as part of an industrial design report.

### 7.8.2 A Harder One: Connections of Specified Length

Imagine two skew lines like  $AB$  and  $CD$  as shown in Fig. 40. Can you connect these with a line segment of specified length? Under what conditions? Under what condition is the connection unique? Given a connecting length greater than this, investigate the nature of the solutions and provide appropriate illustrations to clearly convey the nature of the solution set.

### 7.8.3 Multiple Connections

If the angle between lines  $AB$  and  $CD$  is  $\theta$ , and referring to the type of connection dealt with in section 7.7, describe the conditions, in terms of  $\alpha$ ,  $\beta$  and  $\theta$ , leading to 0, 1, 2, 3 or 4 possible connections. Illustrate your reasoning appropriately.

(LatexCourses)M2DG289LC.tex